

THE ROLE OF HALOGENATED SPECIES IN THE TROPOSPHERE - MODEL CALCULATIONS

Asgeir Sorteberg and Øystein Hov*

Department of Geophysics, University of Bergen
N-5007 Bergen, Norway

1 Introduction

Episodic boundary layer ozone depletion events in the Arctic in spring (Barrie et al., 1988; Bottenheim, 1990; Solberg et al., 1996) put focus on the potential importance of halogens in tropospheric chemistry. Measurements of alkanes, alkenes and alkynes (Jobson et al., 1994; Solberg et al., 1996; Ramacher et al., 1997), formaldehyde measurements (de Serves, 1994), NO_x measurements (Beine et al., 1997) and the possible influence of halogens as a sink of *DMS* (Toumi, 1994) point to the large oxidation capacity of chlorine and bromine compounds.

Few calculations have been made of the role of halogens in the atmospheric boundary layer at mid latitudes (Sander and Crutzen, 1996; Vogt et al., 1996). In this paper we address how halogen chemistry affect the production and loss of ozone and precursors. An extensive gas phase reaction scheme of bromine and chlorine compounds has been added to a simplified hydrocarbon chemistry in order to investigate the possible role of reactive halogen species for 'background' concentrations of the halogens and for elevated halogen levels with subsequent ozone depletion as seen in the Arctic in spring. The background levels are based on measurement at

*Now at the Norwegian Institute for Air Research (NILU)

mid latitude in the HALOTROP project (Platt et al., 1998), and on previous Arctic measurements (Hausmann and Platt, 1994; Tuckermann et al., 1997). These measurements have often been below detection limits, making it difficult to quantify a background level.

The emissions of halogens chosen in the calculations correspond to an upper limit. For the concentrations of nitrogen and hydrocarbon compounds, two cases have been investigated, one case where polluted air with elevated levels of ozone is transported into the marine environment, and a typical clean air case. This choice was done to investigate chemical sources and sinks of the different halogens, and to investigate the effect of halogens on other compounds for two concentration regimes.

Special emphasis has been put on the interaction of bromine and chlorine chemistry and the nonlinearity of the ozone depletion with higher Cl_2 emissions. A release mechanism of bromine from sea salt and an evaluation of maximum release rates and the uncertainties involved are discussed. The possibility of ozone depletion events for different levels of nitrogen, hydrocarbons and ozone is investigated, and the importance of hydrocarbons as a sink of active bromine is discussed. A halogen release mechanism from liquid sea salt aerosols is added to the gas phase chemistry, and in Table 1 there is a summary of the different halogen sources and release mechanisms used in the different simulations.

A simplified *DMS* chemistry where the products of *DMS* oxidation are not considered, is included to investigate the importance of chlorine and bromine as sinks for *DMS*, the role of *DMS*-halogen reactions in ozone depletion through the *DMS/BrO* catalytic cycle, and *DMS* as a sink of active chlorine and bromine compounds.

A 3D numerical model of troposphere chemistry and transport, coupled to a meteorological limited area model, is applied to investigate the competition between chemical and physical processes in the determining the fate of the halogen radicals. The rate of exchange between the atmospheric boundary layer and the free troposphere was quantified. Due to lack of knowledge of the emissions of halogens the emissions were adjusted to correspond to the measured concentrations. The lack of emission data has made it necessary to focus on concentration ratios and on the relative contribution within the group of halogen compounds to reduce the sensitivity of the results to absolute emission rates.

Section	Prescribed gas phase Br_2 emissions		Prescribed gas phase Cl_2 emissions		Br_2 and/or Cl_2 release through HOX scavenging		Br_2 release through OH or NO_3 scavenging	
	yes	no	yes	no	yes	no	yes	no
3	x		x			x		x
4	x		x			x		x
5	x		x			x		x
6.1	x		x		x			x
6.2	x		x		x			x
6.3	x		x		x			x
6.4		x		x	x		x	
7.2	x		x			x		x
7.3	x		x			x		x
7.4	x		x			x		x
7.5	x		x			x		x

Table 1: Emission of halogens used in the different sections. $X = Br$ and Cl .

2 Box model description

2.1 Gas phase chemistry

The gas phase chemistry is listed in Table 2 and consists of an extensive bromine and chlorine chemistry and a simplified hydrocarbon chemistry with lumped species. Ethane represents a typical alkane, ethene a typical alkene and ethyne a typical alkyne. Their concentrations are therefore not directly comparable to observed values, but represent lumped values. Halogen compounds taken into account are Br , Br_2 , BrO , $HOBr$, $BrONO_2$, HBr , $BrCl$, Cl , Cl_2 , ClO , Cl_2O_2 , $HOCl$, $ClONO_2$ and HCl . Special emphasis is made on bromine - chlorine interactions in order to investigate the partitioning between the different halogen compounds, when no heterogeneous or wet phase reactions are involved. Reaction rates have been taken from recent literature. However, products of Br reactions with hydrocarbons are not well known and assumed to be in the form of HBr . Decomposition of $OClO$ to $O(^3P) + ClO$ and XOO ($X = Br$ and Cl) to $X + O_2$ is assumed to be fast. In Figure 1 the halogen containing reactions accounted for in the gas phase are shown.

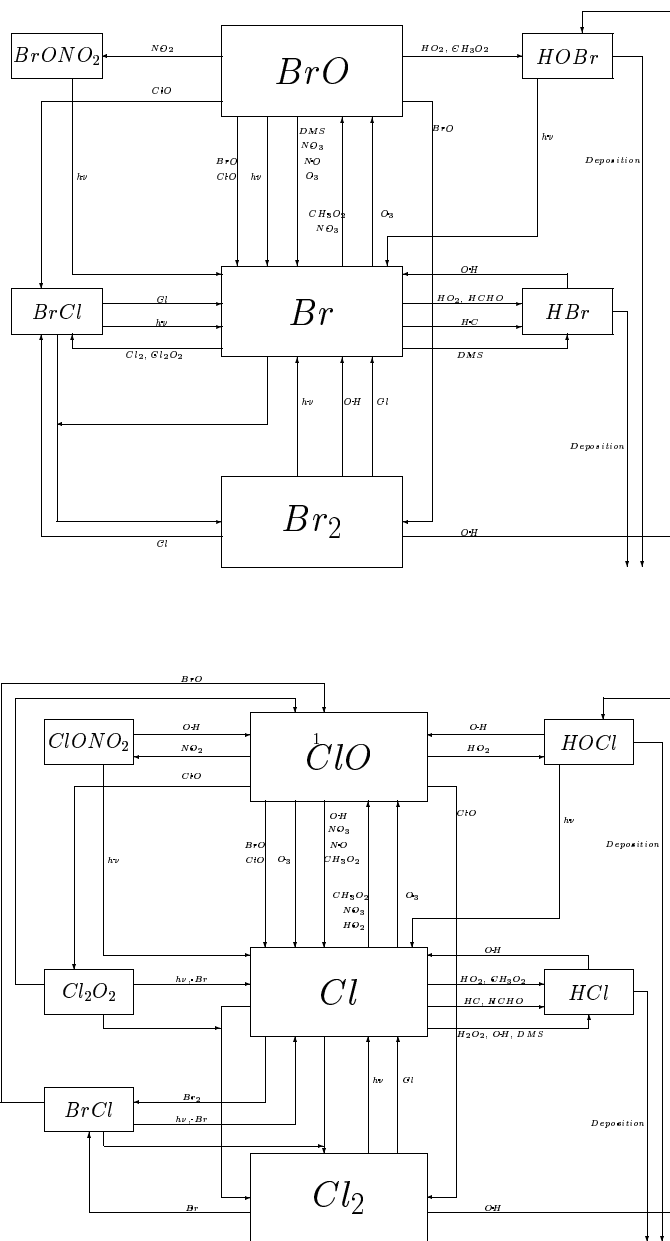


Figure 1: Scheme of bromine and chlorine reactions in the gas phase accounted for in model.

Number	Reaction (of order n)	n	$\frac{K^\theta}{M^{1-n} T^{\theta-1}}$	Reference
G001	$O(^3P) + O_2 \rightarrow O_3$	2	$6.0 \times 10^{-34} (T/300)^{-2.8} O_2$ $5.6 \times 10^{-34} (T/300)^{-2.8} N_2$	Atkinson et al., 1997
G002	$O(^1D) + M \rightarrow O(^3P)$	2	$3.2 \times 10^{-11} O_2^{+70/T}$	DeMore, 1992
G003	$O(^3P) + NO \rightarrow NO_2$	2	$1.8 \times 10^{-11} N_2 \exp(110/T)$ $1.0 \times 10^{-31} (T/300)^{-1.6} N_2 (k_0)$ $3.0 \times 10^{-11} (T/300)^{0.3} (k_\infty)$ $F_c = \exp(-T/1850)$	Atkinson et al., 1997
G004	$H_2O + O(^1D) \rightarrow 2OH$	2	2.2×10^{-10}	Atkinson et al., 1997
G005	$O_3 + NO \rightarrow NO_2$	2	$1.8 \times 10^{-12} \exp(-1370/T)$	Atkinson et al., 1997
G006	$O_3 + NO_2 \rightarrow NO_3$	2	$1.2 \times 10^{-13} \exp(-2450/T)$	Atkinson et al., 1997
G007	$O_3 + OH \rightarrow HO_2$	2	$1.9 \times 10^{-12} \exp(-1000/T)$	Atkinson et al., 1997
G008	$O_3 + HO_2 \rightarrow OH$	2	$1.4 \times 10^{-14} \exp(-600/T)$	Atkinson et al., 1997
G009	$NO + NO_3 \rightarrow 2NO_2$	2	$1.8 \times 10^{-11} \exp(110/T)$	Atkinson et al., 1997
G010	$NO + HO_2 \rightarrow NO_2 + OH$	2	$3.7 \times 10^{-12} \exp(240/T)$	Atkinson et al., 1997
G011	$NO_2 + NO_3 \rightarrow NO + NO_2$	2	$4.5 \times 10^{-14} \exp(-1260/T)$	Atkinson et al., 1997
G012	$NO_2 + NO_3 \rightarrow N_2O_5$	2	$2.7 \times 10^{-30} (T/300)^{-3.4} N_2 (k_0)$ $2.0 \times 10^{-12} (T/300)^{0.2} (k_\infty)$ $F_c = \exp(-T/250)$	Atkinson et al., 1997
G013	$NO_2 + OH \rightarrow HNO_3$	2	$2.6 \times 10^{-30} (T/300)^{-2.5} N_2 (k_0)$ $6.7 \times 10^{-11} (T/300)^{-0.6} (k_\infty)$ $F_c = 0.43$	Atkinson et al., 1997
G014	$NO_2 + HO_2 \rightarrow HO_2NO_2$	2	$1.8 \times 10^{-31} (T/300)^{-3.2} N_2 (k_0)$ $4.7 \times 10^{-12} (k_\infty)$ $F_c = 0.6$	Atkinson et al., 1997
G015	$NO_3 + NO_3 \rightarrow 2NO_2$	2	2.7×10^{-16}	Wayne, 1991
G016	$NO_3 + H_2O_2 \rightarrow HO_2 + HNO_3$	2	2.0×10^{-15}	Wayne, 1991
G017	$N_2O_5 \rightarrow NO_2 + NO_3$	2	$1.0 \times 10^{-3} (T/300)^{-3.5}$ $\exp(-11000/T) N_2 (k_0)$ $9.7 \times 10^{14} (T/300)^{0.1}$ $\exp(-11080/T) (k_\infty)$ $F_c = \exp(-T/250) \exp(-1050)$	Atkinson et al., 1997
G018	$N_2O_5 + H_2O \rightarrow 2HNO_3$	2	1.3×10^{-21}	EMEP
G019	$HO_2NO_2 \rightarrow NO_2 + HO_2$	1	$5.0 \times 10^{-6} \exp(-10000/T) N_2 (k_0)$ $2.6 \times 10^{15} \exp(-10900/T) (k_\infty)$ $F_c = 0.6$	Atkinson et al., 1997
G020	$OH + H_2 \rightarrow HO_2$	2	$7.7 \times 10^{-12} \exp(-2100/T)$	Atkinson et al., 1997
G021	$OH + HO_2 \rightarrow$	2	$4.8 \times 10^{-11} \exp(250/T)$	Atkinson et al., 1997
G022	$OH + H_2O_2 \rightarrow HO_2$	2	$2.9 \times 10^{-12} \exp(160/T)$	Atkinson et al., 1997
G023	$OH + HO_2NO_2 \rightarrow NO_2$	2	$1.5 \times 10^{-12} \exp(360/T)$	Atkinson et al., 1997
G024	$HO_2 + HO_2 \rightarrow H_2O_2$	2	$2.3 \times 10^{-13} \exp(600/T) +$ $1.7 \times 10^{-33} \exp(1000/T) M \times$ $(1. + 1.4 \times 10^{-21} \exp(2200/T) H_2O)$	DeMore, 1992
G025	$OH + HNO_3 \rightarrow NO_3$	2	$7.2 \times 10^{-15} \exp(785/T) +$ $1.9 \times 10^{-33} \exp(725/T) M /$ $(1 + 1.9 \times 10^{-33} \exp(725/T) M /$ $4.1 \times 10^{-16} \exp(1440/T)$	Atkinson et al., 1997
G026	$CH_4 + OH \rightarrow CH_3O_2$	2	$2.3 \times 10^{-12} \exp(-1765/T)$	Atkinson et al., 1997
G027	$CH_4 + NO_3 \rightarrow CH_3O_2 + HNO_3$	2	4.0×10^{-19}	Atkinson et al., 1997
G028	$C_2H_6 + OH \rightarrow CH_3O_2$	2	$7.9 \times 10^{-12} \exp(1030/T)$	Atkinson et al., 1997
G029	$C_2H_6 + NO_3 \rightarrow CH_3O_2 + HNO_3$	2	1.0×10^{-12}	Singh and Zim., 1992
G030	$C_2H_4 + OH \rightarrow CH_3O_2$	2	2.0×10^{-17}	Mallard et al., 1993
G031	$C_2H_4 + O_3 \rightarrow HCHO + 0.42CO$ $+ 0.12HO_2 + 0.12H_2$	2	1.0×10^{-11} $9.1 \times 10^{-15} \exp(-2580/T)$	Singh and Zim., 1992 Atkinson et al., 1997
G032	$C_2H_4 + NO_3 \rightarrow CH_3O_2 + HNO_3$	2	$3.3 \times 10^{-12} \exp(-2880/T)$	Atkinson et al., 1997
G033	$C_2H_2 + OH \rightarrow HCOOH + CO + HO_2$	2	$5.0 \times 10^{-30} \exp(T/300)^{-1.5} N_2 (k_0)$ $9.0 \times 10^{-13} \exp(T/300)^{2.0} (k_\infty)$ $F_c = 0.62$	Atkinson et al., 1997

Number	Reaction (of order n)	n	$\frac{K^\theta}{M^{1-n} s^{-1}}$	Reference
G034	$CO + OH \rightarrow HO_2$	2	$1.3 \times 10^{-13} (1. + 0.6M)(300/T)$	Atkinson et al., 1997
G035	$CH_3O_2 + NO \rightarrow HCHO + HO_2 + NO_2$	2	$4.2 \times 10^{-12} \exp(180/T)$	Atkinson et al., 1997
G036	$CH_3O_2 + CH_3O_2 \rightarrow 2HCHO + 2HO_2$	2	$1.1 \times 10^{-13} \exp(365/T)$	Atkinson et al., 1997
G037	$CH_3O_2 + CH_3O_2 \rightarrow CH_3OH + HCHO$	2	$1.1 \times 10^{-13} \exp(365/T)$	Atkinson et al., 1997
G038	$CH_3OH + OH \rightarrow HCHO + HO_2$	2	$3.1 \times 10^{12} \exp(360/T)$	Atkinson et al., 1997
G039	$CH_3OH + NO_3 \rightarrow HCHO + HNO_3 + HO_2$	2	$1.3 \times 10^{-12} \exp(-2560/T)$	Atkinson et al., 1997
G040	$CH_3O_2 + HO_2 \rightarrow CH_3O_2H$	2	$3.8 \times 10^{-13} \exp(780/T)$	Atkinson et al., 1997
G041	$CH_3O_2H + OH \rightarrow HCHO + OH$	2	$1.0 \times 10^{-12} \exp(190/T)$	Atkinson et al., 1997
G042	$CH_3O_2H + OH \rightarrow CH_3O_2$	2	$1.9 \times 10^{-12} \exp(190/T)$	Atkinson et al., 1997
G043	$HCHO + OH \rightarrow CO$	2	$8.6 \times 10^{-12} \exp(20/T)$	Atkinson et al., 1997
G044	$HCHO + NO_3 \rightarrow CO + HO_2 + HNO_3$	2	5.8×10^{-10}	Atkinson et al., 1997
G045	$HCOOH + OH \rightarrow HO_2$	2	4.5×10^{-13}	Atkinson et al., 1997
G050	$HCl + OH \rightarrow H_2O + Cl$	2	$2.4 \times 10^{-12} \exp(-330/T)$	Atkinson et al., 1997
G051	$Cl + HO_2 \rightarrow HCl + O_2$	2	$1.8 \times 10^{-11} \exp(170/T)$	Atkinson et al., 1997
G052	$Cl + HO_2 \rightarrow ClO + OH$	2	$4.1 \times 10^{-11} \exp(-450/T)$	Atkinson et al., 1997
G053	$Cl + O_3 \rightarrow ClO + O_2$	2	$2.9 \times 10^{-11} \exp(-260/T)$	Atkinson et al., 1997
G054	$Cl + H_2O_2 \rightarrow HCl + O_2$	2	$1.1 \times 10^{-11} \exp(-980/T)$	Atkinson et al., 1997
G055	$Cl + NO_3 \rightarrow ClO + NO_2$	2	2.4×10^{-11}	Atkinson et al., 1997
G056	$Cl + CH_4 \rightarrow HCl + CH_3O_2$	2	$9.6 \times 10^{-12} \exp(-1350/T)$	Atkinson et al., 1997
G057	$Cl + C_2H_6 \rightarrow HCl + CH_3O_2$	2	$8.1 \times 10^{-11} \exp(-95/T)$	Atkinson et al., 1997
G058	$Cl + C_2H_4 \rightarrow HCl + CH_3O_2$	2	$1.6 \times 10^{-29} ((T/300)^{-3.5}) M (k_0)$ $3.0 \times 10^{-10} (k_\infty)$ $F_c = 0.6$	Atkinson et al., 1997
G059	$Cl + C_2H_2 \rightarrow HCl$	2	$5.7 \times 10^{-30} ((T/300) - 3) N_2 (k_0)$ $2.3 \times 10^{-10} (k_\infty)$ $F_c = 0.6$	Atkinson et al., 1997
G060	$Cl + C_2H_2 \rightarrow 2CO + 2HO_2 + Cl$	2	$5.7 \times 10^{-30} ((T/300)^{-3}) N_2$	Atkinson et al., 1997
G061	$Cl + C_2H_2 \rightarrow 2CO + 2HO_2 + Cl$	2	$5.7 \times 10^{-30} ((T/300)^{-3}) N_2$	Atkinson et al., 1997
G062	$Cl + C_2H_2 \rightarrow 2CO + HO_2 + HCl$	2	$5.7 \times 10^{-30} ((T/300)^{-3}) N_2$	Atkinson et al., 1997
G063	$Cl + CH_3OH \rightarrow HCl + HCHO + HO_2$	2	5.5×10^{-11}	Atkinson et al., 1997
G064	$Cl + CH_3O_2 \rightarrow ClO + HCHO + HO_2$	2	1.0×10^{-11}	Assumed
G065	$Cl + CH_3O_2 \rightarrow HCl + CO + H_2O$	2	5.0×10^{-12}	Assumed
G066	$Cl + HCHO \rightarrow HCl + HO_2 + CO$	2	$8.2 \times 10^{-11} \exp(-34/T)$	Atkinson et al., 1997
G067	$Cl + Cl_2O_2 \rightarrow Cl_2 + Cl + O_2$	2	1.0×10^{-10}	Atkinson et al., 1997
G068	$Cl_2 + OH \rightarrow HOCl + Cl$	2	$1.4 \times 10^{-12} \exp(-900/T)$	Atkinson et al., 1997
G069	$ClO + OH \rightarrow HO_2 + Cl$	2	$1.1 \times 10^{-11} \exp(120/T)$	Atkinson et al., 1997
G070	$ClO + OH \rightarrow HCl + O_2$	2	$1.1 \times 10^{-11} \exp(120/T)$	Atkinson et al., 1997
G071	$ClO + HO_2 \rightarrow HOCl + O_2$	2	$4.6 \times 10^{-13} \exp(710/T)$	Atkinson et al., 1997
G072	$ClO + O_3 \rightarrow Cl + 2O_2$	2	1.5×10^{-17}	Atkinson et al., 1997
G073	$ClO + O_3 \rightarrow O(^3P) + ClO + O_2$	2	1.0×10^{-18}	Atkinson et al., 1997
G074	$ClO + NO \rightarrow Cl + NO_2$	2	$6.2 \times 10^{-12} \exp(294/T)$	Atkinson et al., 1997
G075	$ClO + NO_2 \rightarrow ClONO_2$	2	$1.6 \times 10^{-31} (T/300)^{-3.4} N_2 (k_0)$ $2.0 \times 10^{-11} (k_\infty)$ $F_c = \exp(-T/430)$	Atkinson et al., 1997
G076	$ClO + NO_3 \rightarrow Cl + NO_2 + O_2$	2	4.7×10^{-13}	Atkinson et al., 1997
G077	$ClO + NO_3 \rightarrow O(^3P) + ClO + NO_2$	2	4.7×10^{-13}	Atkinson et al., 1997
G078	$ClO + CH_3O_2 \rightarrow Cl + HCHO + HO_2$	2	$4.9 \times 10^{-12} \exp(-330/T)$	Atkinson et al., 1997
G079	$ClO + ClO \rightarrow Cl_2O_2$	2	$1.7 \times 10^{-32} ((T/300)^{-4}) N_2 (k_0)$ $5.4 \times 10^{-12} (k_\infty)$ $F_c = 0.6$	Atkinson et al., 1997
G080	$ClO + ClO \rightarrow Cl_2 + O_2$	2	$1.0 \times 10^{-12} \exp(-1590/T)$	Atkinson et al., 1997
G081	$ClO + ClO \rightarrow 2Cl + O_2$	2	$3.0 \times 10^{-11} \exp(-1590/T)$	Atkinson et al., 1997
G082	$ClO + ClO \rightarrow Cl + O(^3P) + ClO$	2	$3.5 \times 10^{-13} \exp(-1370/T)$	Atkinson et al., 1997
G083	$HOCl + OH \rightarrow ClO + H_2O$	2	$3.0 \times 10^{-12} \exp(-500/T)$	Atkinson et al., 1997
G084	$ClONO_2 + OH \rightarrow ClO + HNO_3$	2	$1.2 \times 10^{-12} \exp(-330/T)$	Atkinson et al., 1997
G085	$Cl_2O_2 \rightarrow ClO + ClO$	1	$1.0 \times 10^{-6} \exp(-8000/T) N_2 (k_0)$ $4.8 \times 10^{15} \exp(-8820/T)$	Atkinson et al., 1997

Number	Reaction (of order n)	n	$\frac{K^{\theta}}{M^{1-n} s^{-1}}$	Reference
G086	$Cl_2O_2 + O_3 \rightarrow ClO + Cl + 2O_2$	2	1.0×10^{-19}	Atkinson et al., 1997
G090	$HBr + OH \rightarrow Br + H_2O$	2	$1.1 \times 10^{-11} (T/298)^{-0.8}$	Atkinson et al., 1997
G091	$Br + O_3 \rightarrow BrO + O_2$	2	$1.7 \times 10^{-11} \exp(-800/T)$	Atkinson et al., 1997
G092	$Br + HO_2 \rightarrow HBr + O_2$	2	$1.4 \times 10^{-11} \exp(-590/T)$	Atkinson et al., 1997
G093	$Br + NO_3 \rightarrow BrO + NO_2$	2	1.6×10^{-11}	Atkinson et al., 1997
G094	$Br + C_2H_4 \rightarrow HBr + CH_3O_2$	2	1.6×10^{-13}	Bierbach et al., 1996
G095	$Br + C_2H_2 \rightarrow HBr + CO + HO_2$	2	$3.6 \times 10^{-14} \times 0.33$	Bierbach et al., 1996
G096	$Br + C_2H_2 \rightarrow Br + 2CO + 2HO_2$	2	$3.6 \times 10^{-14} \text{ times } 0.33$	Bierbach et al., 1996
G097	$Br + C_2H_2 \rightarrow HBr + 2CO + HO_2$	2	$3.6 \times 10^{-14} \text{ times } 0.33$	Bierbach et al., 1996
G098	$Br + CH_3OH \rightarrow HBr + HCHO + HO_2$	2	5.0×10^{-16}	Barnes, 1996
G099	$Br + CH_3O_2 \rightarrow BrO + CO$	2	5.0×10^{-14}	Assumed
G100	$Br + HCHO \rightarrow HBr + CO + HO_2$	2	$1.7 \times 10^{-11} \exp(-800/T)$	Atkinson et al., 1997
G101	$Br + Cl_2O_2 \rightarrow BrCl + Cl + O_2$	2	3.0×10^{-12}	Atkinson et al., 1997
G102	$Br + Cl_2 \rightarrow BrCl + Cl$	2	1.1×10^{-15}	Mallard et al., 1993
G103	$Br_2 + OH \rightarrow HOBr + Br$	2	$1.2 \times 10^{-11} \exp(400/T)$	Atkinson et al., 1997
G104	$Br_2 + Cl \rightarrow BrCl + Br$	2	1.2×10^{-10}	Mallard et al., 1993
G105	$BrCl + Br \rightarrow Br_2 + Cl$	2	3.3×10^{-15}	Mallard et al., 1993
G106	$BrCl + Cl \rightarrow Br + Cl_2$	2	1.5×10^{-11}	Mallard et al., 1993
G107	$BrO + HO_2 \rightarrow HOBr + O_2$	2	$6.2 \times 10^{-12} \exp(500/T)$	Atkinson et al., 1997
G108	$BrO + O_3 \rightarrow Br + 2O_2$	2	5.0×10^{-17}	Atkinson et al., 1997
G109	$BrO + NO \rightarrow Br + NO_2$	2	$8.7 \times 10^{-12} \exp(260/T)$	Atkinson et al., 1997
G110	$BrO + NO_2 \rightarrow BrONO_2$	2	$4.7 \times 10^{-31} (T/300)^{-3.1} N_2 (k_0)$ $1.7 \times 10^{-11} (T/300)^{-0.6} N_2 (k_{\infty})$ $F_c = \exp(-T/327)$	Atkinson et al., 1997
G111	$BrO + NO_3 \rightarrow Br + O_2 + NO_2$	2	1.0×10^{-12}	Atkinson et al., 1997
G112	$BrO + CH_3O_2 \rightarrow Br + HCHO + HO_2$	2	5.7×10^{-12}	LeBras, 1997
G113	$BrO + ClO \rightarrow Br + O(^3P) + ClO$	2	$1.6 \times 10^{-12} \exp(430/T)$	Atkinson et al., 1997
G114	$BrO + ClO \rightarrow Br + Cl + O_2$	2	$2.9 \times 10^{-12} \exp(220/T)$	Atkinson et al., 1997
G115	$BrO + ClO \rightarrow BrCl + O_2$	2	$5.8 \times 10^{-13} \exp(170/T)$	Atkinson et al., 1997
G116	$BrO + BrO \rightarrow 2Br + O_2$	2	$4.0 \times 10^{-12} \exp(-190/T)$	Atkinson et al., 1997
G117	$BrO + BrO \rightarrow Br_2 + O_2$	2	$4.2 \times 10^{-14} \exp(660/T)$	Atkinson et al., 1997
G140	$CH_3SCH_3 + OH \rightarrow SO_2 + 2HCHO$	2	$1.1 \times 10^{-11} \exp(-254/T)$	Atkinson et al., 1997
G141	$CH_3SCH_3 + OH \rightarrow HO_2$	2	$1.7 \times 10^{-12} \exp(7810(1/T - 1/298.))$	Atkinson et al., 1989
G142	$CH_3SCH_3 + NO_3 \rightarrow SO_2 + 2HCHO + NO_2$	2	$1.9 \times 10^{-13} \exp(520/T)$	Atkinson et al., 1997
G143	$CH_3SCH_3 + Cl \rightarrow SO_2 + 2HCHO + HCl$	2	9.0×10^{-15}	Atkinson et al., 1997
G144	$CH_3SCH_3 + Br \rightarrow SO_2 + 2HCHO + HBr$	2	2.7×10^{-13}	Atkinson et al., 1997
G145	$CH_3SCH_3 + BrO \rightarrow Br$	2	$1.5 \times 10^{-14} \exp(845/T)$	LeBras, 1996
G150	$SO_2 + OH \rightarrow HO_2 + Sulphate$	2	$4.0 \times 10^{-30} (T/300)^{-3.3} N_2 (k_0)$ $2.0 \times 10^{-12} (k_{\infty})$ $F_c = 0.45$	Atkinson et al., 1989

Table 2: Gas phase reactions included in the model.

In the calculations the anthropogenic NMHC emissions were represented (by volume) as 45% ethane, 30% ethene, 10% ethyne, 10% methanol and 5% formaldehyde.

The photolysis rates are calculated for a typical mid latitude spring/summer atmosphere (Anderson et al., 1986) with a background aerosol load using a albedo of 0.1 and no cloud conditions. The program used is the Phodis program package (Kylling et al., 1995) which calculates photodissociation rates in the wavelength range 116-850 *nm* with optional cloud and aerosol calculations. The radiative transfer calculations are done for three regions, including 202.5-850.0 *nm*, with multiple scattering to account for O_2 , O_3 , Rayleigh scattering and optional water clouds, cirrus clouds and aerosols. The handling of multiple scattering may be done in different ways in the Phodis package. In this calculation a two-stream algorithm was used (Kylling et al., 1995). Absorption cross sections were collected from the literature. Typical daytime photolysis rates are given in Table 3.

Number	Reaction	$\frac{J}{s-T}$	Reference
J01	$O_3 \rightarrow O(^1D)$	3.1×10^{-5}	DeMore et al., 1992
J02	$O_3 \rightarrow O(^3P)$	5.0×10^{-4}	DeMore et al., 1992
J03	$H_2O_2 \rightarrow 2.OH$	7.4×10^{-6}	DeMore et al., 1992
J04	$NO_2 \rightarrow O(^3P) + NO$	8.9×10^{-3}	DeMore et al., 1992
J05	$NO_3 \rightarrow NO$	2.6×10^{-2}	DeMore et al., 1992
J06	$NO_3 \rightarrow NO_2 + O(^3P)$	2.0×10^{-1}	DeMore et al., 1992
J07	$N_2O_5 \rightarrow NO_2 + NO_3$	4.5×10^{-5}	DeMore et al., 1992
J08	$HNO_3 \rightarrow NO_2 + OH$	6.0×10^{-7}	DeMore et al., 1992
J09	$HO_2NO_2 \rightarrow HO_2 + NO_2$	2.7×10^{-6}	DeMore et al., 1992
J10	$CH_3O_2H \rightarrow HCHO + OH + HO_2$	5.1×10^{-6}	DeMore et al., 1992
J11	$HCHO \rightarrow CO + 2.HO_2$	2.9×10^{-5}	DeMore et al., 1992
J12	$HCHO \rightarrow CO + H_2$	4.6×10^{-5}	DeMore et al., 1992
J20	$HOCl \rightarrow Cl + OH$	2.4×10^{-4}	Atkinson et al., 1997
J21	$Cl_2O_2 \rightarrow 2Cl + O_2$	1.3×10^{-3}	Atkinson et al., 1997
J22	$ClONO_2 \rightarrow Cl + NO_3$	5.0×10^{-5}	Atkinson et al., 1997
J23	$Cl_2 \rightarrow 2Cl$	2.4×10^{-3}	Atkinson et al., 1997
J30	$HOBr \rightarrow Br + OH$	2.0×10^{-3}	Rattigan et al., 1996
J31	$BrONO_2 \rightarrow Br + NO_3$	1.0×10^{-3}	Atkinson et al., 1997
J32	$Br_2 \rightarrow 2Br$	3.4×10^{-2}	Atkinson et al., 1997
J33	$BrCl \rightarrow Br + Cl$	1.1×10^{-2}	Atkinson et al., 1997
J34	$BrO \rightarrow Br + O(^3P)$	3.8×10^{-2}	Atkinson et al., 1997

Table 3: Photolysis rates in the gas phase. (Noon, no cloud values at 45°N, ozone column of 350 DU).

Dry deposition velocities are given in Table 4 and were held constant during the box model runs.

Species	Sea	land
O_3	0.02	0.5
H_2O_2	0.2	0.5
HO_2	0.2	0.2
NO_2	0.2	0.6
NO_3	0.1	0.5
N_2O_5	0.1	0.5
HNO_3	0.5	2.0
CH_3O_2H	0.5	0.5
CH_3O_2	0.2	0.2
$HCHO$	0.2	0.5
HCl	0.5	1.0
$HOCl$	0.2	0.2
HBr	0.5	1.0
$HOBr$	0.2	0.2
SO_2	0.4	0.8

Table 4: Dry deposition velocities (cm/s) over sea and land.

3 Bromine and chlorine gas phase chemistries and their interactions

Box model calculations were done with prescribed halogen emissions in order to investigate the influence of gas phase bromine and chlorine chemistry on ozone at different halogen emission rates.

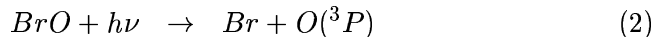
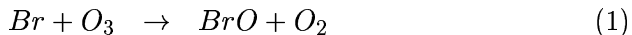
The scenarios represent polluted air and relatively clean air. Table 5 gives the emissions and initial concentrations used in the runs. A scenario of polluted air was performed by assuming that a parcel of air was advected over land for three days exposed to emissions (see Table 5) and thereafter entering into the marine environment without emissions of non-halogenated species and with constant emissions of Br_2 and Cl_2 for five days. In addition a clean air scenario was performed by assuming a parcel of air being in a marine environment for five days without any emission of non halogenated species and constant emissions of Br_2 and Cl_2 . All emissions were assumed to be instantaneously mixed in the boundary layer with a height of 1000 m.

species	Initial conc.		emissions	
	clean	polluted	over land	over sea
O_3	30	40	0	0
H_2O_2	2.0	2.0	0	0
NO	0.1	0.2	5.0×10^{11}	0
NO_2	0.2	0.5	0	0
HNO_3	0.1	0.1	0	0
CO	100	200	1.4×10^{11}	0
H_2	500	500	0	0
SO_2	0.1	0.2	1.4×10^{11}	0
CH_4	1700	1700	0	0
C_2H_6	2.0	3.0	$0.45 * 1.0 \times 10^{12}$	0
C_2H_4	1.0	1.0	$0.30 * 1.0 \times 10^{12}$	0
C_2H_2	0.2	1.0	$0.10 * 1.0 \times 10^{12}$	0
CH_3OH	0.5	1.0	$0.10 * 1.0 \times 10^{12}$	0
$HCHO$	0.1	1.0	$0.05 * 1.0 \times 10^{12}$	0
DMS	0	0	0	0
Cl_2	0	0	0	1.0×10^{10}
Br_2	0	0	0	3.5×10^8

Table 5: Initial concentrations (*ppb*) and emissions (molecules $cm^{-2}s^{-1}$) used in the box model calculations.

Several calculations were done with different emission rates ranging from 3.5×10^8 molecules $cm^{-2}s^{-1}$ (0.5 ppt/h) to 1.0×10^{10} molecules $cm^{-2}s^{-1}$ (15 ppt/h). Figure 2 shows the reduction of ozone with increased Br_2 emissions after two and five days in the polluted and clean air case. Peak BrO concentration calculated within the five days ranged from 2.9 and 4.5 ppt in the polluted and clean air cases, respectively, to 45.3 and 46.7 ppt for zero chlorine emissions. It is seen that in the absence of chlorine the rate of destruction increase with increasing Br_2 emission.

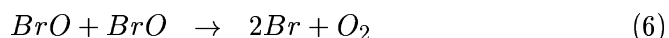
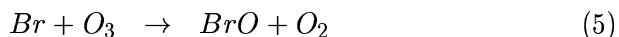
Ozone destruction by bromine mainly takes place in reactions with bromine radicals where Br atoms are oxidized by ozone to BrO and where most of the BrO will photolyse back to Br and $O(^3P)$ with no net effect on ozone,





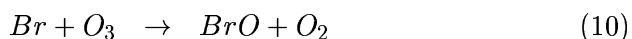
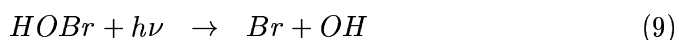
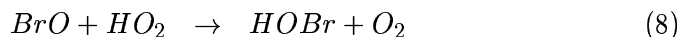
However, in several chain reactions BrO is converted to Br without producing oxygen atoms and there is a net ozone loss.

A Br/BrO catalytic cycle was suggested by Barrie et al., 1988:

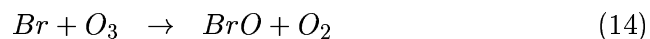
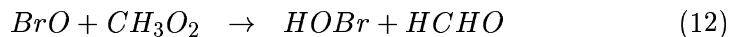


where the BrO self reaction is the rate limiting step. A branch of the BrO self reaction produces Br_2 instead of Br with a rate which is about 15 times slower at 288 K.

In the presence of peroxides $HOBr$ is formed and converted to Br by photolysis,



and a similar pathway was recently pointed out for CH_3O_2

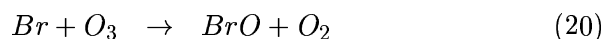
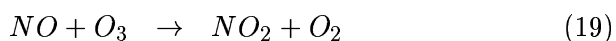
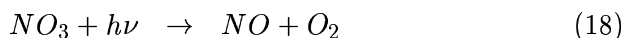
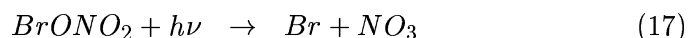


The reaction rate coefficient of BrO with CH_3O_2 is about the same as for HO_2 .

In a possible branch of the $BrO + HO_2$ reaction HBr and O_3 may be formed. This branch is not accounted for in the scheme, but if it exists it influences the partitioning of reactive and unreactive bromine greatly. Garcia and Solomon (1994) examined the effect of different branching and found the BrO abundance to depend critically on the yield of HBr . Comparisons between model calculations and observations suggested a yield substantially

less than 5%. Laboratory measurements by Poulet et al., 1992 pointed out the fact that HBr is a possible product of the $BrO + HO_2$ reaction, but suggested a negligible yield at 298 K. Mellouki et al., 1994 suggested that at most 0.01% of the $BrO + HO_2$ reaction would give HBr as a product.

Burkholder et al., 1995 pointed out that if $BrONO_2$ photolysis produced NO_3 and Br an effective $BrONO_2$ cycle may exist through:

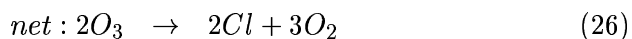
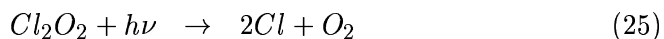
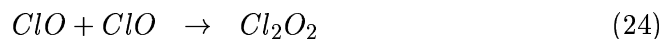
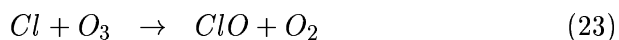


where either photolysis of $BrONO_2$ or of NO_3 is the rate limiting step. However the products of $BrONO_2$ photolysis is rather uncertain, and if BrO and NO_2 are produced instead of Br and NO_3 the cycle will be a null cycle.

Calculations where Cl_2 emissions ranged from 1.0×10^{10} molecules $cm^{-2}s^{-1}$ (15 ppt/h) to 8.0×10^{10} molecules $cm^{-2}s^{-1}$ (120 ppt/h), were done to investigate the influence of chlorine chemistry on the bromine compounds and on the ozone depletion. Peak ClO concentrations ranged from 11 and 26 ppt in the polluted and clean air cases (15 ppt/h Cl_2 emissions), respectively, to 88 and 68 ppt with an emission rate of 120 ppt/h of Cl_2 and no bromine emissions. Several calculations were done with different levels of Br_2 and Cl_2 . When bromine emissions were added the ClO concentrations dropped significantly due to the reactions with BrO .

Figure 2 shows that the role of Cl_2 emissions is more complicated than the role of bromine. The formation of ClO will influence the ozone destruction in a quite nonlinear way.

The ozone destruction rate increases through the photolysis of Cl_2 :



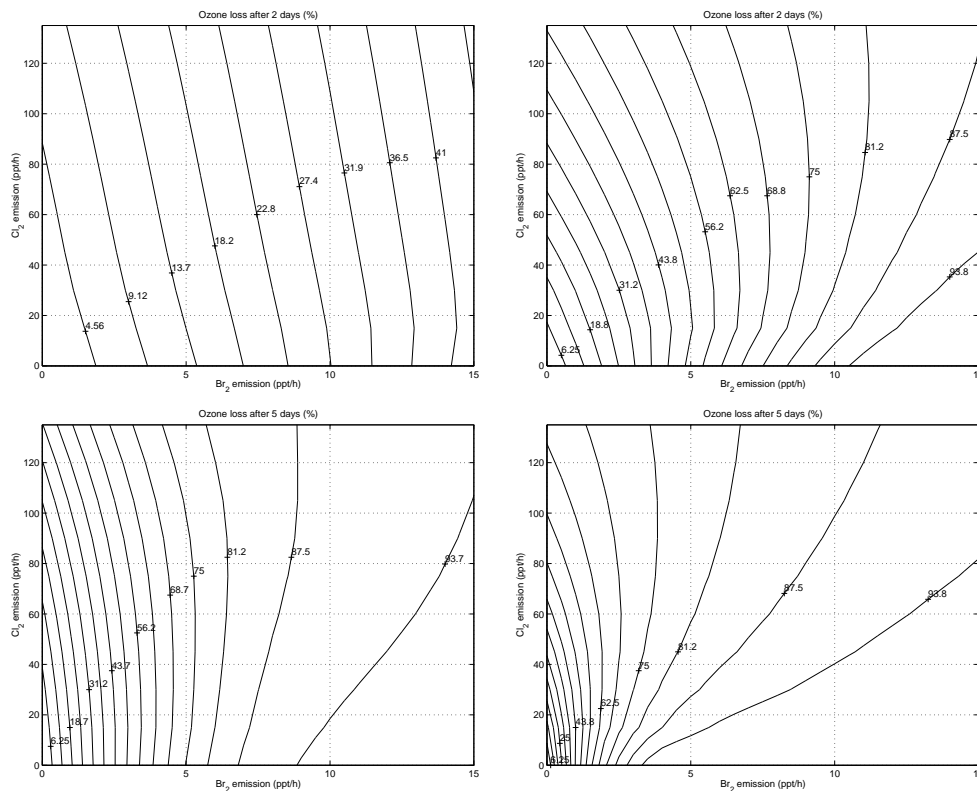
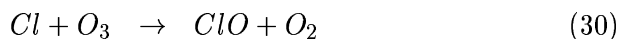
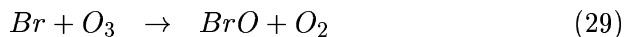
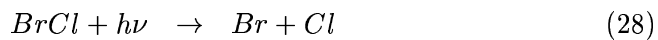
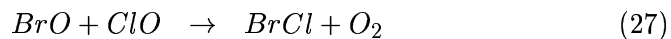


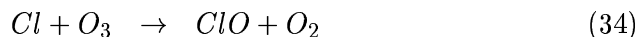
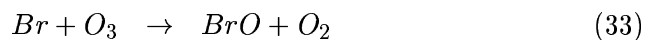
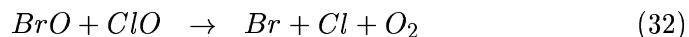
Figure 2: Isolines for ozone loss in % compared to a case with zero halogen emissions after 2 and 5 days of emissions of Br_2 and Cl_2 in the polluted (left) and clean air case (right).

There are several less important reaction products of the ClO self reaction (See Table 2).

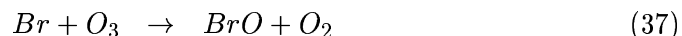
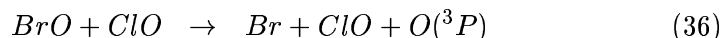
The chlorine compounds will also affect the destruction efficiency of Br through the coupling of BrO and ClO through three different routes:



where below 15 km formation of $BrCl$ is the rate limiting step (Lary, 1996). This cycle is about six times slower than the alternative cycle:

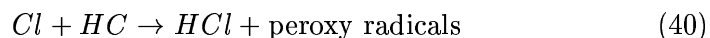


One branch of the $BrO + ClO$ reaction gives ClO and $O(^3P)$, which is almost as fast as the cycle above. This cycle gives no net ozone loss:

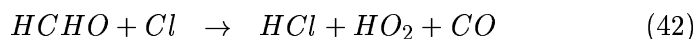


In the two latter cycles the rate limiting step is the $BrO + ClO$ reaction.

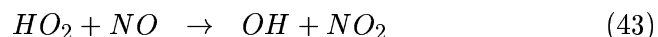
The $BrO + ClO$ reaction 35 is about three times faster than the BrO self reaction which means that even if small amounts of ClO is present the $BrO + ClO$ reactions may be important. This may reduce the ozone destruction efficiency of $BrO + BrO$ in favour of $BrO + ClO$ which at most will give one Br and one Cl atom. Even if the reaction rate coefficient of Cl with ozone is higher than that of Br , there are more competing reaction pathways for Cl due to its higher reactivity with hydrocarbons.

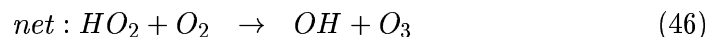
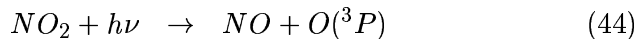


which may reduce the total ozone depletion compared to the case of no Cl_2 emission. In addition to be a sink of reactive Cl the reactions with hydrocarbons may also increase the peroxide concentration which may have one of two effects on the ozone concentration:

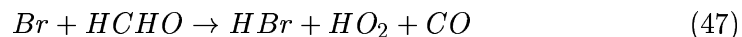


HO_2 can then be converted by NO into OH and produce a further molecule of ozone:





or remove ozone through the $HO_2 + O_3$ reaction. The importance of these reactions depends on the NO_x level. Chlorine compounds will greatly influence the $HCHO$ concentration through the enhancement of peroxides (eg. reaction 41). The increase in $HCHO$ can reduce the effect of bromine induced ozone destruction since a greater portion of the bromine will be in an unreactive form through



From Figure 2 it is seen that the depletion of ozone is nonlinear when Cl_2 and Br_2 act together. This is especially the case in the clean air scenario.

4 The role of halogen chemistry in the troposphere

Field measurements in mid latitudes (Platt et al., 1998) showed very low BrO and ClO concentrations, mostly below the detection limits (~ 2.5 ppt for BrO and ~ 14 ppt for ClO). However, a few samples had concentration slightly above the detection limit.

Box model calculations with gas phase bromine and chlorine chemistry in addition to conventional oxidant chemistry were done to investigate the influence of gas phase halogen chemistry on ozone and precursors in a marine environment.

The scenarios represent polluted air and relatively clean air with Br_2 and Cl_2 emissions estimated in order to keep the BrO and ClO concentrations close to the maximum observed values. This should correspond to an upper limit influence of a 'background' concentration of these two compounds. Initial concentrations and emissions are different in the two cases and are given in Table 5.

In the polluted air scenario it was assumed that a parcel of air was advected over land for three days with emissions (Table 5) and then it passed over a marine area with no emissions of non-halogenated species and with a constant emission of 3.5×10^8 (0.5 ppt/h) and 1.0×10^{10} molecules

$cm^{-2}s^{-1}$ (15 ppt/h) of Br_2 and Cl_2 , respectively for five days. In the clean air case there were no emission of non halogenated compounds. All emissions were assumed to be instantaneously mixed in the boundary layer with a height of 1000 m.

The Br_2 and Cl_2 emissions were kept the same in the two cases to compare the effect of gaseous halogen chemistry on other trace gases at different concentration levels.

Average ClO concentrations were 1.3 and 4.5 ppt in the polluted and clean air cases, respectively. In Figure 3 it is seen that the ClO concentration in clean air peaks at 2-3 times the polluted case peak because in the polluted case the concentrations of hydrocarbons which react with Cl is higher and less Cl is available for conversion to ClO through the reaction with ozone. There is also a faster loss of ClO through the reaction with HO_2 in the polluted case. The BrO concentration on the other hand does not show this difference due to a substantially less influence of the hydrocarbons on the Br concentration and the increased production of BrO in the polluted case due to higher ozone concentrations is balanced by a higher loss through HO_2 and CH_3O_2 compared to the clean air case. On average BrO concentrations were 0.9 and 1.0 ppt in the polluted and clean air cases, respectively. The main sinks of BrO are photolysis and reaction with HO_2 and production is by reaction with ozone.

There is a difference in the other bromine species, however. The production of $HOBr$ in the clean air case is about 2/3 of the pollutant case due to less HO_2 in the clean air case. The lower ozone concentration in the clean air case implies that more Br is available for reaction with hydrocarbons to create HBr . Due to higher NO_2 concentrations in the polluted case the production of $BrONO_2$ is substantially higher than in the clean air case. The NO_2 level in the calculation with polluted air is not more than ~ 4 ppb as the parcel enters the marine environment. NO_2 concentrations substantially higher than this may be found in a polluted air mass, and this will enhance the production of $BrONO_2$ on the expense of $HOBr$. Due to reaction of NO_2 with BrO and ClO the NO_x concentrations were substantially lowered in the case of halogen emissions compared to a run with no halogens. The relative effect was most pronounced in the clean air case and suggests that halogens then are an important sink for NO_2 .

The concentration of ethane and ethyne was reduced by 15 and 24 %, respectively in the polluted case, and 55 and 77 % in the clean air scenario,

after five days (Table 6) compared to a calculation that did not include halogens. The average net loss rate of C_2H_6 and C_2H_2 is 0.34 and 0.17 ppb/day in the polluted case and 0.44 and 0.019 ppb/day in the clean air case due to reaction of C_2H_6 and C_2H_2 with Cl . There was also a small reduction in H_2O_2 due to the $Cl + H_2O_2$ reaction.

There is also an increase in the CH_3O_2 concentration due to Cl reaction with CH_4 and other hydrocarbons compared to a calculations without any halogen emissions (see Figure 4). The CH_3O_2 self reaction causes in the clean air case, an 80% increase in the $HCHO$ concentration after five days compared to the run with no halogen emissions. This is also due to the Cl reaction with CH_3OH , CH_3O_2 and ClO reaction with CH_3O_2 .

Specie	Polluted case			Clean air case		
	with halogens	no halogens	ratio	with halogens	no halogens	ratio
NO_x	0.022	0.011	1.95	0.0070	0.0010	6.75
C_2H_6	9.9	11.6	0.85	0.5	1.0	0.45
C_2H_2	2.8	3.7	0.76	0.028	0.12	0.23
HO_2	27.8	28.2	0.98	13.9	14.7	0.94
CH_3O_2	26.5	28.5	0.93	16.1	17.5	0.92
$HCHO$	0.71	0.59	1.22	0.28	0.16	1.79
O_3	63.2	69.7	0.91	15.4	21.0	0.73

Table 6: Concentrations (ppb and ppt for HO_2 and CH_3O_2) and differences in concentration at daytime (12 GMT) between the run with halogens and without (with halogens/without) after five days in a marine environment.

In Figure 3 it is seen that the halogen emissions have a larger relative effect on the ozone concentration in the clean air case with a 27% reduction in ozone after five days, compared to a run with no halogen emissions. The effect on ozone in the polluted case was 9% (Table 6). In absolute values the effect was almost equal in the polluted and clean air cases. Average net ozone loss rate due to the halogens was 1.3 and 1.1 ppb/day in the polluted and clean air cases, respectively.

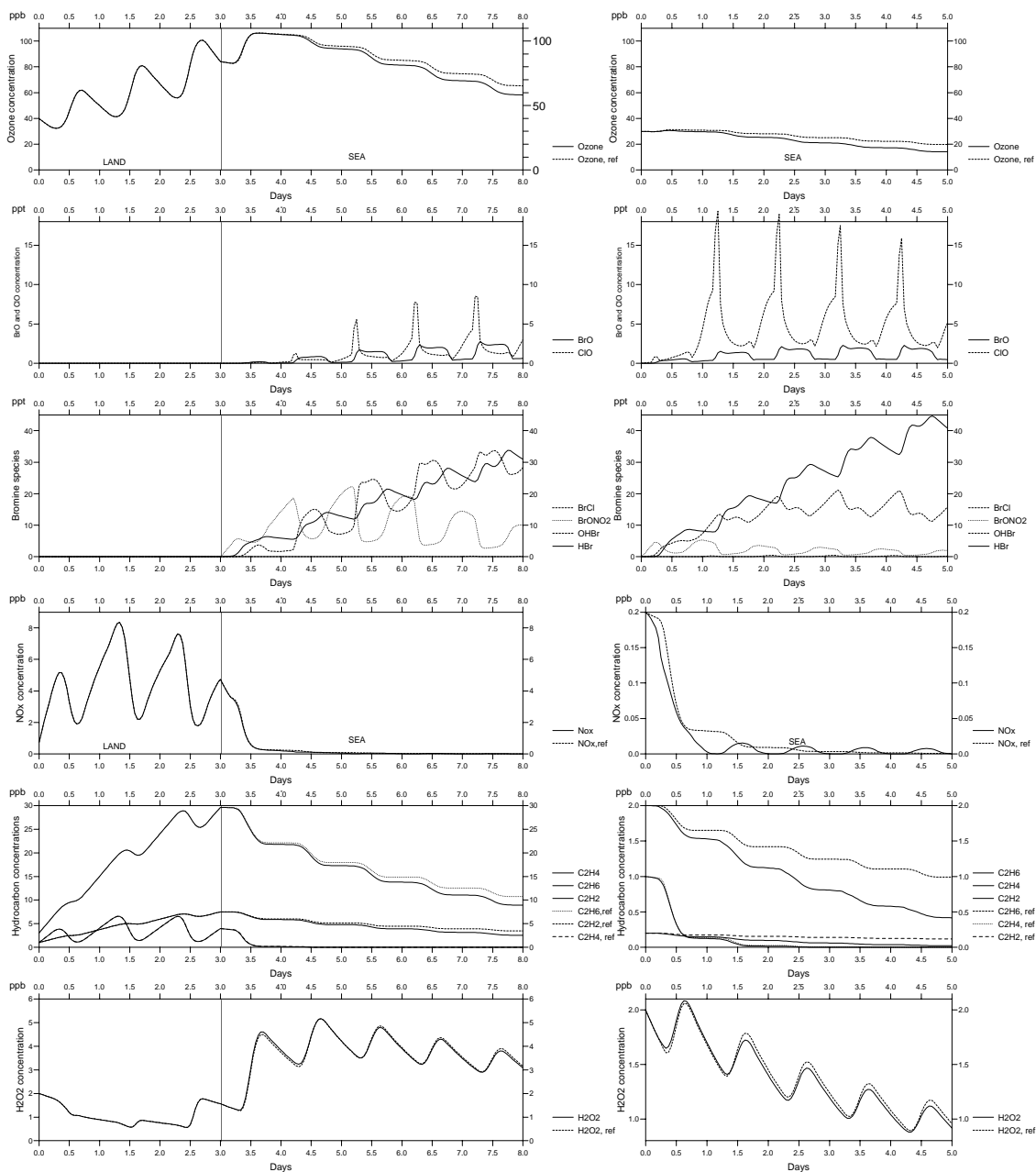


Figure 3: The concentration of different chemical compounds for a polluted (left) and clean air (right) case compared to a run with no emission of Br_2 and Cl_2 (ref).

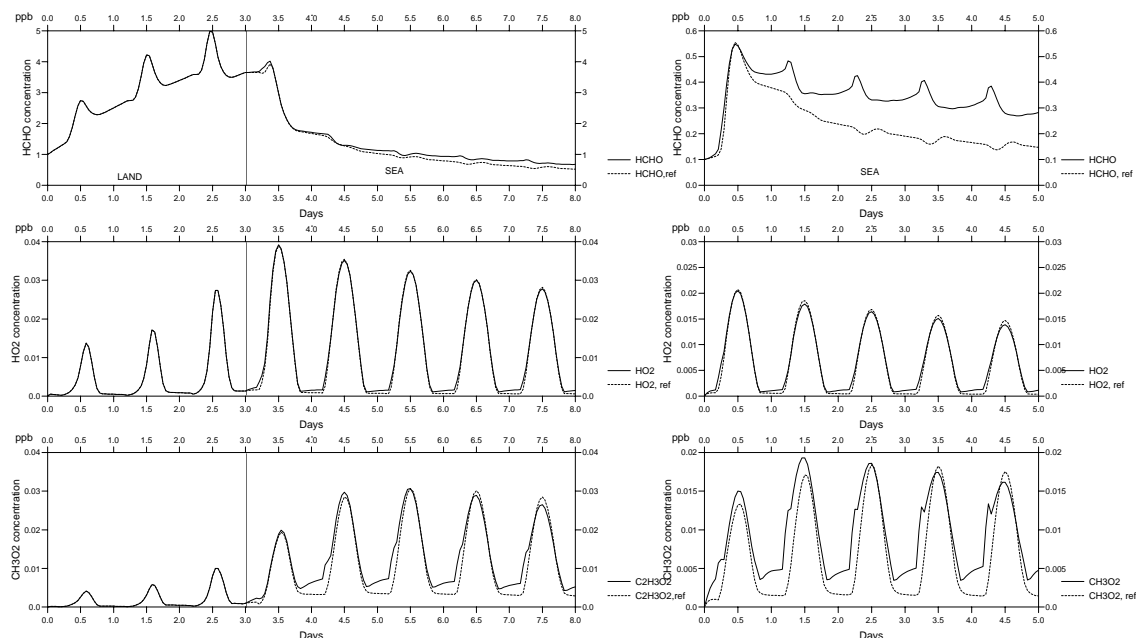


Figure 4: The concentration of different chemical compounds for a polluted (left) and clean air (right) case compared to a run with no emission of Br_2 and Cl_2 (ref).

In order to investigate the net effect of different halogen reactions on the destruction of ozone in events of low halogen emissions several runs were performed where one or more halogen reactions was left out and the ozone loss compared to a run with no halogens. Figure 4 shows the cumulative ozone loss in ppb due to halogens compared to a run with no halogens. It is clearly seen that the main ozone loss is due to the $Br + O_3$ reaction both in the polluted and clean air case. If this reaction is removed the ozone loss by halogens after five days at sea would only be 1 and 2 ppb in the polluted and clean air case, respectively. Also the $BrO + HO_2$ reaction is a main ozone loss mechanism with a net contribution of 3 and 1.3 ppb, respectively. However the $BrO + NO_2$ reaction is seen to be unimportant as a ozone depleter in the clean air case and actually slightly suppress the ozone destruction in the polluted case. This is surprising bearing in mind the $BrONO_2$ catalytic cycle described in reaction 21, but without the $BrO + NO_2$ reaction more BrO is available to react with HO_2 to make

$HOBr$ which is photolysed to Br more rapidly than does $BrONO_2$.

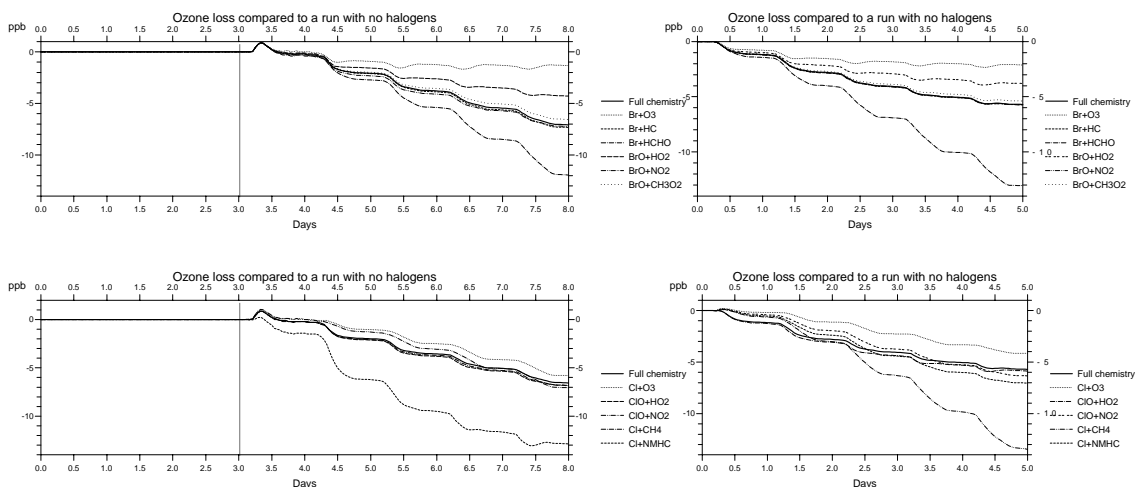


Figure 5: Ozone loss (ppb) when one halogen reaction was left out at a time compared to the run with no halogen emissions (left: polluted case, right: clean air case).

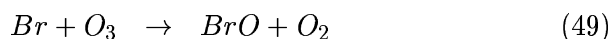
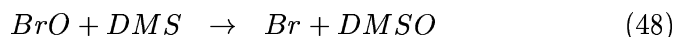
The main bromine reaction that acts as a suppression of ozone destruction is the Br reaction with $HCHO$ to make unreactive HBr . In the clean air case over twice the amount of ozone was depleted when this reaction was not taken into account. Reactions of Br with $NMHC$ s had little effect on the ozone depletion when the halogen emissions were small. The reaction $Cl + O_3$ is the main ozone destruction mechanism involving chlorine and is in particular important in the clean air case where less chlorine is lost by reactions with hydrocarbons. The $Cl + NMHC$ reactions have little effect in clean air since loss of reactive Cl to HCl is then mainly by reaction with methane. In the polluted case the main loss of Cl is through $NMHC$ reactions. Leaving out these reactions in the polluted case will double the ozone loss. In the clean air case excluding the $Cl + CH_4$ reaction gives lower ozone destruction the first day because less CH_3O_2 is produced. This gives lower HO_2 concentrations since the CH_3O_2 self reaction is reduced. Lower HO_2 gives lower ozone destruction in this case since the $HO_2 + O_3$ reaction is an important loss mechanism for ozone.

It should be noted that these results are from a box model calculation

with no natural or anthropogenic sources of $NMHC$ or NO_x at sea, or horizontal or vertical advection within the boundary layer. A five days residence time of the air parcel over sea is a long time, and most of these assumptions enhance the role of the halogen compounds. These calculations therefore represent an upper limit of how halogen emissions may influence other species, and the chemical influence investigated here may in many circumstances be hidden by more important physical processes.

5 The role of bromine as a sink of DMS

Calculations were performed where emissions of dimethylsulphide (DMS) was included to investigate the role of bromine as a sink of DMS . In the presence of DMS ozone may be depleted through DMS oxidation by BrO to create $DMSO$ (Barnes et al., 1991; Toumi, 1994).



the fate of $DMSO$ is not considered in the model.

Figure 6 shows the pronounced effect of chlorine and bromine emissions on the DMS concentrations both in the polluted and clean air case. This shows the importance of halogens in oxidizing DMS .

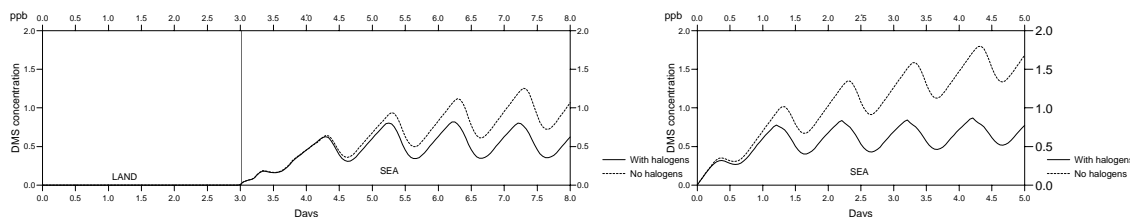


Figure 6: Halogens act as a sink of DMS . Br_2 and Cl_2 emissions over the sea are 3.5×10^8 molecules $cm^{-2}s^{-1}$ (0.5 ppt/h) and 1.0×10^{10} molecules $cm^{-2}s^{-1}$ (15 ppt/h), respectively. The polluted case to the left and clean air case to the right.

DMS may also act as a sink of active bromine through reaction with Br to produce HBr . This reaction is more than ten times slower than the

reaction of BrO with DMS at 288 K. In addition DMS acts as a sink of active Cl . Calculated concentration of DMS of about 0.5 ppb reduced the ozone loss to about one half compared to calculations without DMS . DMS can therefore be an important sink of active halogens.

6 Possible release through liquid sea salt aerosols - Model calculations

Several possible emission sources of halogens have been proposed: release from algae and other microbiological activities (Schall et al., 1994; Barrie et al., 1988; Sturges et al., 1992, Li et al., 1994; Class et al., 1986), activation of sea salt bromine in aerosols (Sander and Crutzen, 1996; Mozourkewich, 1995) or accumulated on the ice shelf (McDonnell et al., 1992).

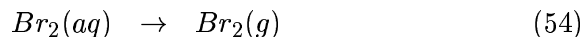
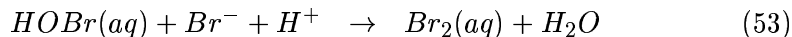
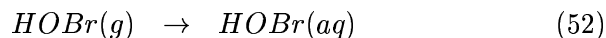
6.1 Autocatalytic release - A possible bromine explosion

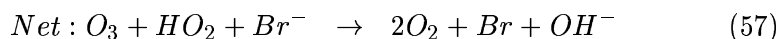
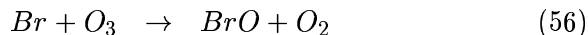
The depletion of halogens in marine aerosols relative to bulk sea water is indirect evidence for a net transport of halogens from the aerosols to the gas phase (Cicerone, 1981). Several authors (eg: Sander and Crutzen 1996) have proposed sea salt aerosols to be a source of bromine through reaction involving $HOBr$ in the aqueous phase.



where Br_2 rapidly gasses out due to its low solubility.

This is a mechanism similar to the heterogenous reaction proposed by Fan and Jacob, 1992. The exception is that while the heterogenous reaction proposed by Fan and Jacob recovers HBr and $HOBr$ lost from the gas phase this cycle may also serve as a source for bromine through the release of sea salt Br^- . The result is conversion of one active bromine specie $HOBr$ into Br_2 that may photolyse to two Br .

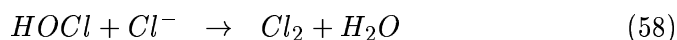




Another source of bromine and chlorine is required to give $HOBr$ in the gas phase. This source is here taken as the 'background' emission of 3.5×10^8 molecules $cm^{-2}s^{-1}$ (0.5 ppt/h) of Br_2 and 1.0×10^{10} molecules $cm^{-2}s^{-1}$ (15 ppt/h) of Cl_2 , which gave average BrO concentrations of 0.9 and 1.0 ppt in the polluted and clean air case, respectively, and 1.3 and 4.5 ppt of ClO in section 4.

The effectiveness of the ozone depletion cycle starting with reaction 52 is dependent on HO_2 , hydrocarbons, aerosol loading and pH. If $HOBr$ is produced in the first place, the pH is low and the loss of active bromine through hydrocarbon reactions is small, a catalytic cycle can be initiated that may deplete significant amounts of ozone.

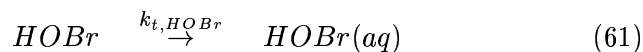
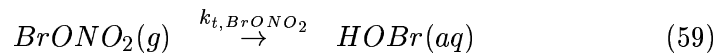
In a similar reaction, $HOCl(aq) + Cl$ reacts to produce Cl_2 that will volatilize from the aqueous phase.



where Cl_2 will gas out.

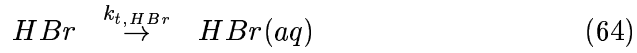
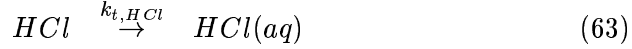
6.1.1 Parameterization of the autocatalytic sea salt release

An upper estimate of the effect of sea salt aerosol scavenging and release by reactions 51 and 58 is evaluated by assuming that $HOCl$, $ClONO_2$, $HOBr$ and $BrONO_2$ which all are rather soluble, are scavenged with a transfer rate k_t , by liquid sea salt aerosols to form



and that $ClONO_2$, $HOCl$, $BrONO_2$ and $HOBr$ immediately form Cl_2 and Br_2 , respectively through reaction with Cl^- and Br^- provided by

scavenging of HCl and HBr that dissolve,



or by Cl^- and Br^- ions that are continuously available in new sea salt aerosols. In other words the liquid sea salt aerosols can act both as a source of and to recycle inactive halogens to active compounds. It is assumed here that the transfer from gaseous to aqueous phase is the rate limiting step and that reactions in the the aqueous phase are instantaneous and give gas phase Cl_2 and Br_2 .

A schematic picture of the simplified treatment of the aerosol scavenging and release of halogens is given in Figure 7.

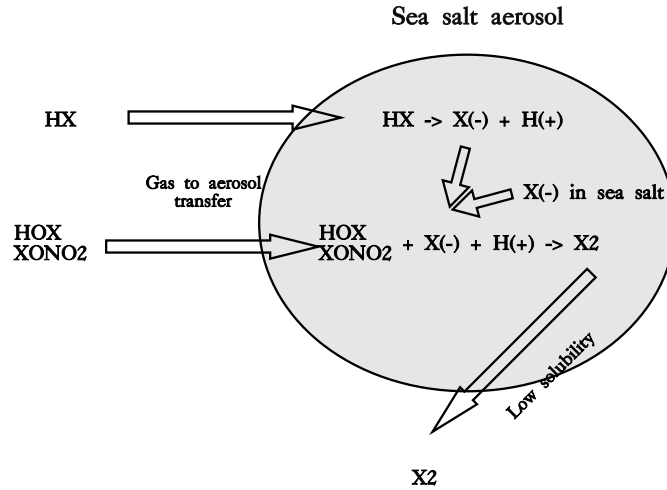


Figure 7: Release mechanism of halogens through liquid sea salt aerosols ($X = Cl$ or Br).

The transfer of molecules from the gas phase to the aqueous phase is treated as a first order loss.

$$\frac{d[C_i(g)]}{dt} = -L_w k_{t,r} C_i(g) \quad (66)$$

were $k_{t,r}$ is the transfer coefficient (s^{-1}) for an aerosol with radius r and L_w is the liquid water volume fraction. It is here assumed that once the gaseous

compound has been transferred into the droplet it does not volatilize back into the gas phase. In other words the transfer is not limited by the effective Henry's law constant, only by the rate of transfer into the aerosol. This assumption is used because the Henry's law coefficients for several of the bromine compounds are not yet known. The halogen compounds which are assumed to be scavenged are believed to be quite soluble, and this supports the simple treatment of this process which gives an upper limit of the loss by aerosol scavenging.

The transfer coefficient k_t describes the mass transport from the bulk gas into the aerosol and can be divided into two steps: Diffusion of gaseous species from bulk gas to the surface of the aerosol and transfer across the gas-liquid interface and can be written as (Schwartz, 1986):

$$k_{t,r} = \left(\frac{r^2}{3\eta D_{gi}} + \frac{4r}{3\bar{v}_i \alpha_i} \right)^{-1} \quad (67)$$

where the first term describes the gas phase diffusion and the second the mass transport across the gas-aqueous interface. D_g is the gas phase diffusivity of species i . Several semi-empirical equations exist in the literature (Sherwood et al., 1975; Marrero and Mason, 1972; Lugg, 1968). By introducing the mean free path λ , D_g can be estimated as $D_g = \lambda\bar{v}/3$. r is the aerosol radius, η is a coefficient correcting for free molecular effects (Fuchs and Sutugin, 1971), α_i the accommodation coefficient of species i defined as the fraction of the incoming molecules that is incorporated into the liquid (sticking coefficient) and \bar{v} the mean molecular speed for specie i given by the Maxwell-Boltzmann distribution:

$$\bar{v} = \sqrt{\frac{8RT}{M_i \pi}} \quad (68)$$

where M_i is molar mass of species i and R given in $ergK^{-1}mol^{-1}$ gives \bar{v} in cms^{-1} . Note that equation 67 implicitly assumes that the accommodation coefficient α not only describes the probability for a transition from the gas to the aqueous phase, but also the probability for transition in the opposite direction. This means that small values of α do not represent a low solubility, only a slow equilibration.

Very little quantitative information is available regarding the accommodation coefficients of $HOBBr$, HBr , $BrONO_2$, $HOCl$ and $ClONO_2$ on water droplets. The accommodation coefficient of HCl is measured to be 0.056 (van

Doren et al., 1990). The other compounds are thought to have coefficients of the same magnitude and a value of 0.01 is assumed.

The dependence of the mass transfer rate coefficient on the accommodation coefficient is displayed in Figure 8. For values where the transfer coefficient is nearly constant with respect to the accommodation coefficient the mass transfer is diffusion controlled, whereas in the range where the transfer coefficient is decreasing with decreasing accommodation coefficient the mass transfer is collision controlled.

It is seen that our choice of accommodation coefficient and aerosol radius greatly influences the transfer rate.

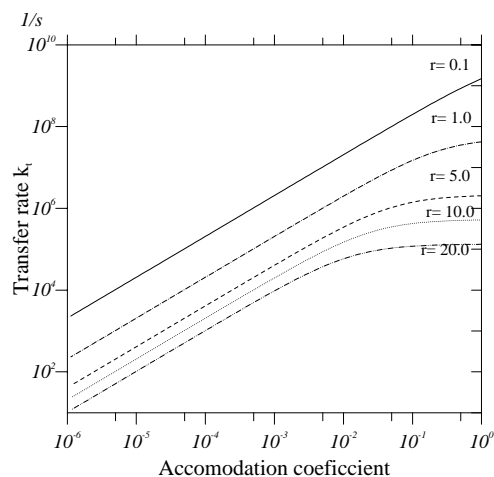


Figure 8: The transfer rate coefficient k_t of $HOBr$ as a function of the accommodation coefficient α and aerosol radius r (μm) with a mean free path of $0.065 \mu m$. The coefficient correcting for free molecular effects (η) is assumed to be 1 and the temperature 288 K.

To assume that the gas to aqueous phase transfer is the limiting step, is a considerable simplification of the aqueous phase chemistry, and gives an upper estimate of the importance of the release of halogens to the gas phase through liquid sea salt aerosols. A more detailed presentation is given by Sander and Crutzen, 1996.

In Figure 9 is shown the ozone loss for different liquid water contents.

It shows that loss of ozone occurs when the transfer rate from gas into the aerosol is fast enough and the pH is sufficiently low for reaction 51 to be the main loss mechanism for $HOBr$. There seems to be no real difference in the course of the depletion events for the clean and the polluted case with equal gas to aerosol transfer rates.

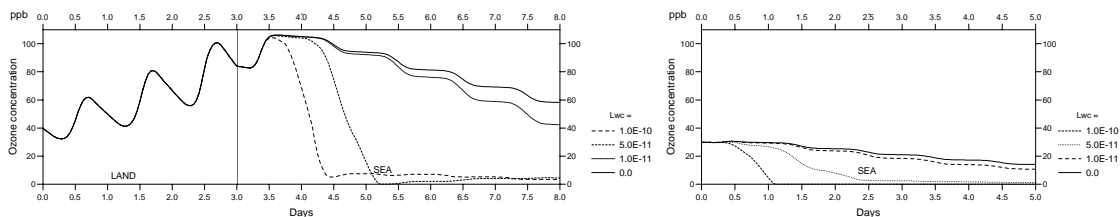


Figure 9: Ozone depletion when $HOBr$ in the aerosols is immediately transformed to Br_2 ($HOBr \rightarrow HOBr(aq) \rightarrow Br_2$) under different aerosol loads (Lwc) in the polluted (left) and clean air case (right).

To investigate the difference in maximum BrO concentration in the polluted and clean air cases during a total ozone depletion event a liquid water content of $5.0 \cdot 10^{-11}$ was assumed to simulate a total loss of ozone in 24 hours. From Figure 10 it is seen that the maximum BrO concentration in the polluted case is more than a factor of three higher than that in the clean air case because more ozone has to be depleted, enhancing the $Br + O_3$ reaction. This is, however, partly compensated by larger loss through the photolysis of BrO , self reaction and reaction with HO_2 .

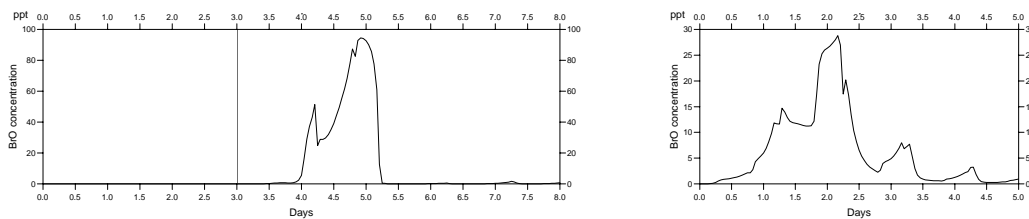


Figure 10: BrO concentrations with a liquid water content (Lwc) of 5.0×10^{-11} in the polluted (left) and clean air case (right).

Figure 10 also shows that even if there is about five times more ozone in the polluted case, the depletion time is about the same as in the clean air case. This is due to higher HO_2 concentrations in the polluted case which gives a higher production of $HOBr$ and therefore a faster recycling through the aerosols. When ozone is depleted the catalytic cycles stop since the production of BrO will be reduced and the production of $HOBr$ through the $BrO + HO_2$ reaction slows down.

Only a small peak of ClO was calculated in the polluted case (3 ppt), due to a large loss through reaction with BrO , and Cl loss by reaction with hydrocarbons. The ClO peak in the clean air case on the other hand was almost 4 times higher. The low ClO concentrations arise because the accommodation coefficients for the chlorine and bromine compounds are set equal (except for HCl), and this gives a scavenging of the chlorine compounds which may be too slow compared to that of bromine.

6.2 Bromine sinks and reservoirs of bromine compounds - bromine reactions with volatile organic compounds

Atmospheric bromine species are relatively short lived. Terminating steps involving formation of HBr through reaction of Br with $HCHO$, HO_2 and alkenes are therefore not as effective as the terminating step in the Cl/ClO cycle and the NO/NO_2 cycle where HCl and HNO_3 are formed, respectively. Bromine catalytic cycles may therefore proceed for a longer time. HBr is the longest lived BrO_y reservoir with a lifetime in the order of a day in a sunlit mid latitude environment and longer at higher latitudes in winter due to less sunlight. HBr is lost through reaction with OH , through dry deposition and through scavenging by precipitation and aerosols.

In the chemical mechanism used the bromine-hydrocarbon reactions lead to unreactive HBr that can only be activated by reaction with OH and by scavenging into sea salt aerosols and consequent Br_2 release. The production of HBr through reactions with hydrocarbons are uncertain, however, and unstable hydrocarbons containing bromine may be formed instead. They may dissociate and form reactive Br . This will greatly enhance the bromine ozone destruction potential. Figure 11 shows the destruction of ozone under the assumption that the reactions of bromine with hydrocarbons produce hydrocarbons containing bromine which imme-

diately dissociates to produce Br instead of HBr .

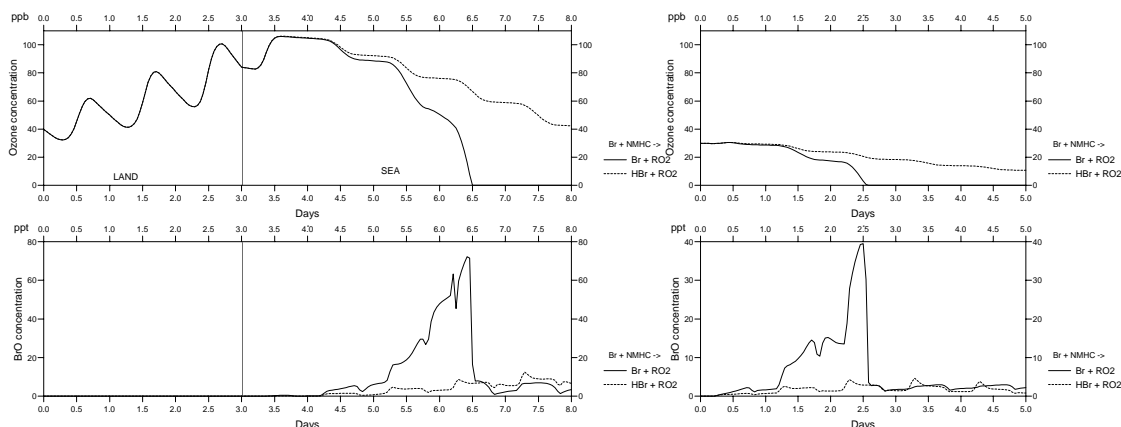
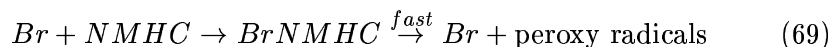


Figure 11: Ozone depletion if the $Br + NMHC$ reactions lead to intermediate products that break up and give Br back, and $HOBBr$ taken up in aerosols immediately is transformed to Br_2 ($HOBBr \xrightarrow{k_t} HOBBr(aq) \xrightarrow{fast} Br_2$), $Lwc=1.0 \times 10^{-11}$.

With a liquid water content of $1.0 \cdot 10^{-11}$ and the $Br + MNHC$ reactions produce HBr , the catalytic ozone depletion cycles were suppressed. If Br is produced (through dissociation of bromine containing hydrocarbons) the catalytic chains may proceed for a longer time, and in this case total ozone depletion resulted. This clearly shows the importance of reactivation of the bromine compounds. It is seen that the relative importance of the Br loss through reaction with hydrocarbons is similar in the polluted and clean air case. This may seem odd taken into account the much higher concentrations of hydrocarbons in the polluted case. But the amount of ozone to deplete is also much higher, therefore more Br must be produced to obtain total ozone depletion. So even if the loss of Br by reaction with hydrocarbons is substantially higher in the polluted case the relative importance of this loss mechanism is more dependent on the hydrocarbon to ozone ratio than on the actual hydrocarbon concentration level.

6.3 DMS during an ozone depletion event

Calculations were done where emissions of *DMS* were added and an ozone depletion event simulated by sea salt scavenging of halogens as explained in section 6.1.1. *DMS* was depleted rapidly by the high *Cl* and *Br* concentrations during the ozone depletion event. Low concentrations of *DMS* should therefore be expected during ozone depletion events.

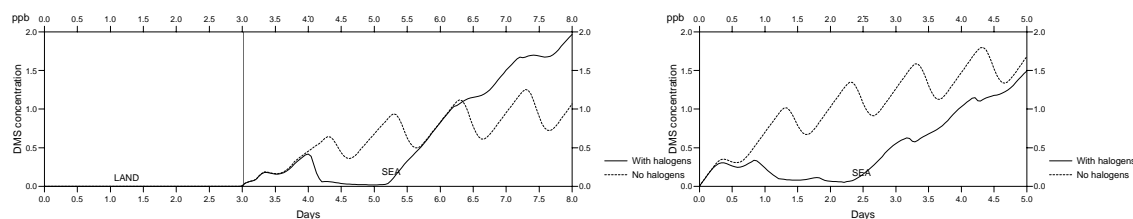


Figure 12: The influence of a total ozone loss on *DMS* in the polluted (left) and clean air (right) case. Liquid water content (Lwc) taken as 5.0×10^{-11} .

From Figure 12 it is seen that when ozone is depleted, the *DMS* concentration will build up rapidly due to reduced *OH* concentrations and therefore only a slow loss of *DMS* through the *OH* + *DMS* reaction. *OH* is reduced since there are little production of *OH* when ozone is small, and due to the buildup of *HBr* after total ozone destruction which reduces the *OH* concentration through the *OH* + *HBr* reaction.

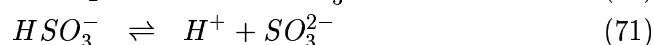
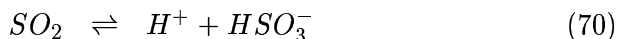
6.4 What may ignite the bromine explosion ?

Since the bromine explosion through reaction 51 assumes a source of gas phase *HOBr*, reaction 51 cannot explain the bromine release without other mechanisms.

6.4.1 The role of sulphur oxidation and Caro's acid

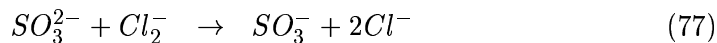
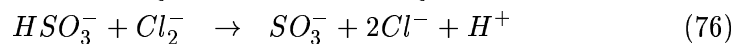
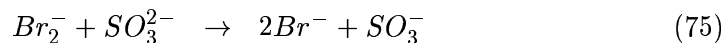
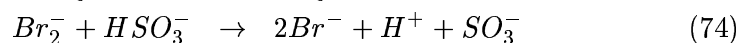
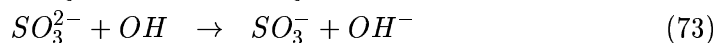
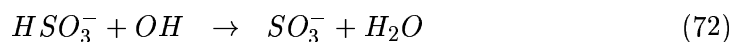
Initially pH in droplets released from seaspray is determined by HCO_3^- in equilibrium with gas phase CO_2 . This gives a pH of about 9. If SO_2 is present *S(IV)* ($\text{SO}_2 + \text{HSO}_3^- + \text{SO}_3^{2-}$) will control the pH through the

equilibria:



As SO_3^{2-} and HSO_3^- are oxidized by O_3 and H_2O_2 to form SO_4^{2-} the pH will drop. This will influence the partitioning between the $S(IV)$ compounds, and thereby the rest of the liquid phase chemistry.

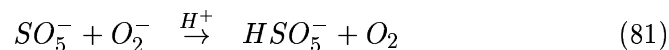
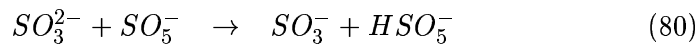
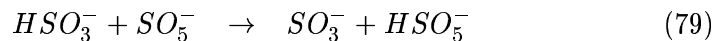
How long the pH will remain high is determined by the $S(IV)$ oxidation, but will generally drop within a few minutes (Chameides and Stelson, 1992). The uptake of gas phase acids may be considered negligible during this initial period. $S(IV)$ may also be oxidized by free radicals such as OH , Cl_2^- and Br_2^- to produce sulphite radicals SO_3^- .



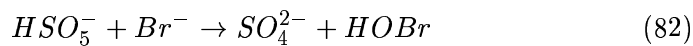
The sulphite radicals will rapidly react with O_2 to form SO_5^- .



SO_5^- may react with HSO_3^- , SO_3^{2-} and O_2^- to form Caro's acid HSO_5^-

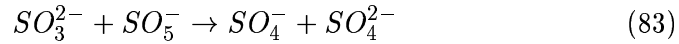


The Caro's acid may then react with halide ions



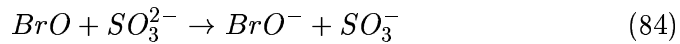
which will lead to Br_2 via reaction of $HOBr$ with Br^- (reaction 51). Br_2 will rapidly gas out due to low solubility. HSO_5^- may also react with SO_3^{2-} to create SO_4^{2-} . This reaction is faster than the Br^- reaction, but with

a decline in the pH the concentration of SO_3^{2-} will drop and this reaction becomes less important (the $H_2SO_5 + HSO_3^-$ reaction is much slower). Also SO_5^- may react with SO_3^{2-} to form SO_4^- and SO_4^{2-} .



In short the amount of Caro's acid is determined by the alkalinity and the competition between reactions producing H_2SO_5 , reaction 83 and O_3 oxidation of SO_3^{2-} .

At 20°C both reaction 83 and O_3 oxidation of SO_3^{2-} dominates the reactions producing H_2SO_5 (Deister and Warneck, 1990; Chameides and Stelson, 1992), however this is not the case at lower temperatures, where Mozourkewich (1995) estimated the reaction ratio of reaction 82 to 83 to be 11 at 240 K. If 20% of the alkalinity is converted to Caro's acid, this will release practically all bromine from the droplet (Mozourkewich, 1995). It should be noted that if BrO is capable of oxidizing SO_3^{2-} at a fast enough rate to compete with reevaporation, this could greatly enhance the H_2SO_5 production



Mid latitude temperatures will not favour production of $HOBr$ through reaction 82 making bromine release by Caro's acid less probable in mid latitudes.

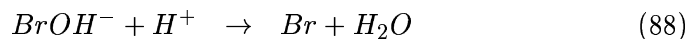
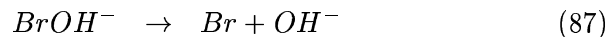
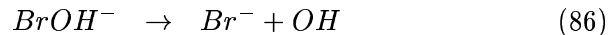
6.4.2 Release through free radical reactions

In addition to possible bromine release by Caro's acid Br_2 may be produced by radical radical reactions under moderate pH conditions as proposed by Mozourkewich, 1995.

The OH radical reacts rapidly with halide ions through XOH^- radicals ($X = Cl$ or Br), eg.:



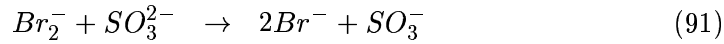
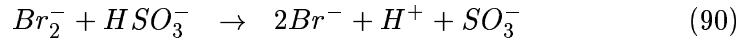
which has 3 major sinks



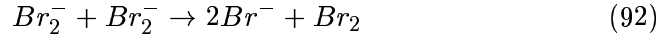
The rate constant coefficients of reaction 87 is $4.2 \cdot 10^6 \text{ s}^{-1}$ and for reaction 88 $4.4 \cdot 10^{10} \text{ M}^{-1}\text{s}^{-1}$ this means that the production of Br will be larger than the Br^- production at pH levels below 3.5 (reaction rate of reaction 86 is $3.3 \cdot 10^7 \text{ s}^{-1}$). Br is rapidly converted to Br_2^- through the equilibrium:



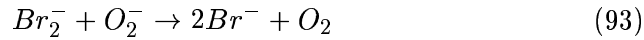
which is shifted to the left ($K_H = 9.1 \cdot 10^{-6}$). The fate of Br_2^- is highly pH dependent. For high pH values the concentration of HSO_3^- and SO_3^- will be high due to higher solubility, and oxidation of HSO_3^- and SO_3^{2-} by Br_2^- will prevent a buildup of Br_2^- concentration.



If, however, the pH is low the main sink will be through



with a reaction rate coefficient of $1.9 \cdot 10^9 \text{ M}^{-1}\text{s}^{-1}$. Another possible sink for Br_2^- is reaction with HO_2 . The products of this reaction are uncertain but are either $2Br^- + H^+ + O_2$ (Sander and Crutzen, 1996) or $Br_2 + HO_2^-$ (Mozourkewich, 1995), in the last case the only reaction that will not create Br_2 is



with a reaction rate of $1.7 \cdot 10^8 \text{ M}^{-1}\text{s}^{-1}$.

6.4.3 Parameterization of the bromine release from free radical reactions

It is argued that at moderate pH levels release of bromine through radical - radical reactions may take place. The aqueous phase chemistry and rate constants are uncertain, but an estimate of the source strength of the mechanism may be derived by assuming that every OH radical scavenged into the aerosol will react with Br^- in the sea salt aerosol and immediately create a Br_2 molecule that volatiles. It is assumed that a continuous production of sea salt aerosols will provide new Br^- ions. The rate limiting step is then:



where k_t is calculated from reaction 67 with an accommodation coefficient for OH on liquid droplets of 0.0035 (Hanson et al., 1992).

Figure 13 shows the production of Br and BrO under the assumptions made above and a liquid water content of 5.0×10^{-11} . No compounds other than OH are scavenged.

It is seen that the production of Br and BrO is quite small even under these favorable conditions (< 0.1 ppt). Calculations with higher liquid water contents were performed to see if the increased gas to liquid transfer rates could initiate an ozone depletion event. This was not the case and we may therefore conclude that under the OH concentrations calculated here, scavenging of OH alone is not sufficient to give enough bromine release to initiate an ozone depletion event. It should be noted that aqueous phase production of OH is not taken into account.

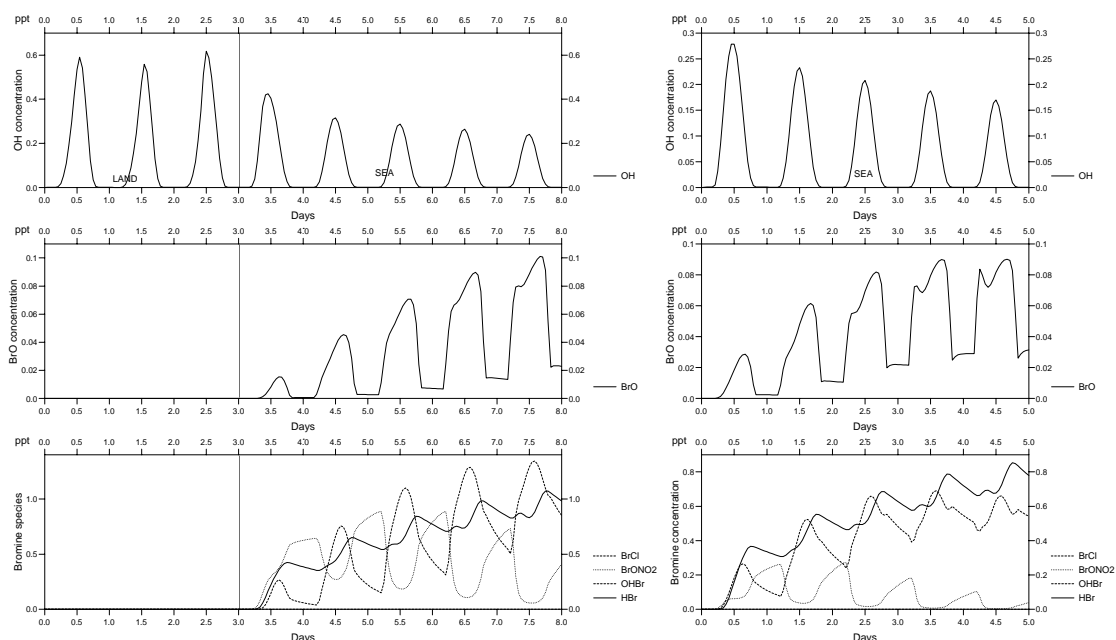


Figure 13: Production of Br , BrO and other bromine compounds by scavenging of OH and consequent Br_2 release in the polluted (left) and clean air case (right). $Lwc=5.0 \times 10^{-11}$.

In order to investigate if the emission of Br_2 by scavenging and aqueous

phase reactions of OH is sufficient to start the bromine catalytic cycles through $HOBr$, scavenging of $HOBr$, HBr and $BrONO_2$ as described in section 6.1.1 is added. A liquid water content of 5.0×10^{-11} was chosen which in the case with 'background' emissions of bromine and chlorine (Table 5) gave nearly total ozone depletion (see Figure 14). Now there is no 'background' emissions, instead the initial release is simulated by the OH scavenging. Figure 14 shows that the initial small release of Br_2 by OH may be enough to start the catalytic ozone depletion both in the polluted and clean air cases. The buildup of BrO is larger in this case than in the case of prescribed chlorine and bromine 'background' emissions. This is due to the fact that in this case only release of bromine is investigated, thus we have no chlorine present and the loss of BrO through the BrO/ClO cycles is zero. The BrO concentration is therefore probably significantly overestimated, but since the BrO/ClO cycles also will lead to ozone loss this will probably not affect that ozone is depleted. This run shows that the initial release of bromine to produce $HOBr$ does not need to be very large to start catalytic release of bromine from the sea salt aerosols by reactions involving $HOBr$. In other words the possibility of an ozone depletion event depends more on how fast $HOBr$ is scavenged into the sea salt aerosol and reacts to create Br_2 in the aqueous phase, than on the absolute source strength of the initial bromine release. The main source of Br_2 through aqueous phase reactions of $HOBr$ is significant if the pH is favorable for the $HOBr + Br^-$ reaction to be the main loss of $HOBr$ in the aqueous phase. However, a low initial source strength will reduce the possibility of an ozone depletion event since the halogen concentrations will be diluted with time and ozone may be advected into the area. The time to deplete ozone is longer in this case than in the case where larger 'background' emissions initiated the autocatalytical bromine release. It should be emphasized that these runs are made under the assumption that scavenging of the gas phase compounds is the rate limiting step and that the pH is favorable for Br_2 producing reactions in the aqueous phase over several days.

6.4.4 NO_3^- initiated release

Large NO_3 gas concentrations in the air (continental air coming over the ocean), may initiate the release of bromine. The gas phase NO_3 will partly

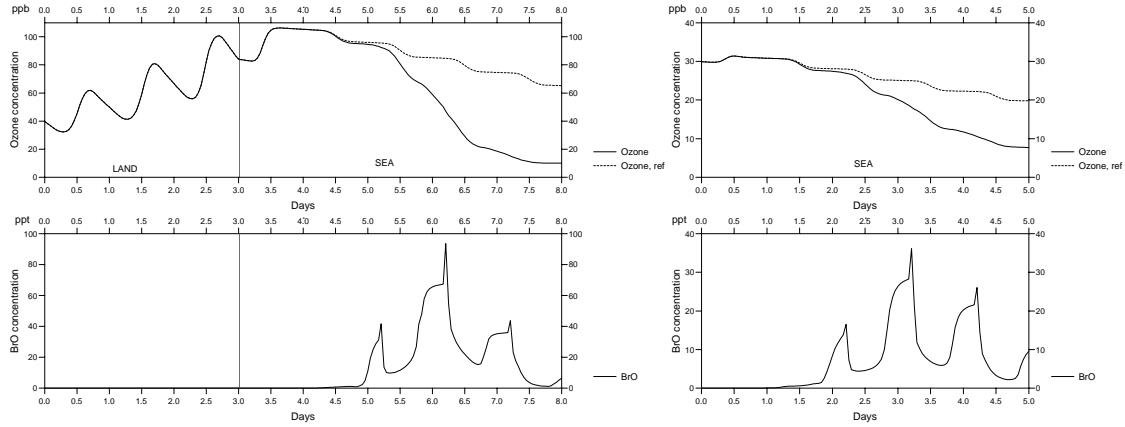
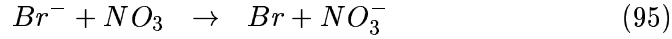


Figure 14: Ozone depletion in the polluted (left) and clean air (right) case when OH , $HOBr$ and $BrONO_2$ are taken up in the sea salt aerosols and are assumed immediately to produce Br_2 . $Lwc=5.0 \times 10^{-11}$. No prescribed emissions of bromine or chlorine.

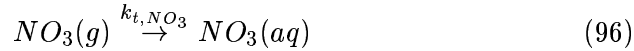
be scavenged by aerosols and oxidized bromine through:



where the Br atom will be in equilibrium with Br_2^- (reaction 89) which will selfreact to Br_2 (reaction 92) under favourable conditions.

6.4.5 Parameterization of release of Br initiated by NO_3^-

The maximum strength of reaction 95 may be investigated by assuming that every NO_3 molecule scavenged into the aerosol will react with Br^- in the sea salt aerosol and eventually create a Br_2 molecule that will volatilize. The rate limiting step is then:



with an accommodation coefficient of 0.0025 (Thomas et al., 1993).

Due to the short lifetime of NO_3 in the gas phase, this source of bromine will be most active for continental air just passing into a marine environment, and may act as an initial source to activate other depletion mechanisms. Runs were done similar to the ones done in section 6.4.2, but with

NO_3 instead of OH as the initial source of bromine. This runs showed that bromine release through NO_3 may activate the $HOBr$ aqueous phase cycle in much the same manner as showed in section 6.4.2 for OH . Runs with high liquid water contents showed that NO_3 scavenging is not fast enough to initiate an ozone depletion event without the additional $HOBr$ scavenging.

7 Model calculations with the UiB 3-D model

The fate of the halogens released in the marine environment was investigated by implementing the gas phase chemistry scheme in Table 2 in a 3-D model and calculations were done for the period 30 April - 10 May 1997 which coincides with measurements done at Mace Head (see section 8).

Since both source strength and origin are not well known, these calculations will only indicate the effect of halogens. The relative importance of the different physical and chemical processes involved is emphasized. The partitioning among the different halogen compounds will be discussed.

7.1 Model description

The Mesoscale Chemistry Transport (MCT) model is developed at the University of Bergen (Flatøy, 1994). It is an Eulerian weather prediction-chemistry model with 10 unequally spaced vertical layers up to 100 hPa with a horizontal grid resolution of 150 km at 60° N. The general approach used in the model is similar to that of the regional acid deposition model RADM (eg. Chang et al., 1987) developed at NCAR. Special attention is made to the treatment of stratiform and convective cloud and precipitation processes (Flatøy, 1992).

The meteorological data necessary to run the model are provided by a weather prediction model (NWP) based on the limited area model Lam50 from the Norwegian Meteorological Institute (Grønås et al., 1987 and Nordeng, 1986). The NWP model has an extended treatment of clouds and precipitation (Sundqvist, 1988, Sundqvist et al., 1989 and Kvamstø, 1992) which gives precipitation data with a high resolution both in time and space. Especially important is a vertical precipitation profile which makes it possible to distribute wet removal vertically.

The physical exchange processes are treated as advection and diffusion.

Transport in convective updrafts and wet and dry removal are described. A second order version of the advection scheme proposed by Bott (1989) is used to solve the advective part. By using a method by Strand and Hov (1993) the Bott scheme can be used in sigma coordinates with variable spacing in the vertical.

The diffusive part is solved using a semi implicit Crank-Nicholson scheme centered in time with an eddy diffusion coefficient K_z with a parameterization based on the stability in the atmospheric boundary layer. For the surface layer (lowest model level) K_z is given as

$$K_z = ku_*z(1 - \frac{z}{h})^2 / B(\frac{z}{L}) \quad (97)$$

where k is von Karman's constant, u_* the friction velocity and B the non-dimensional concentration profile given by Businger's function (Businger et al., 1971) which vary with stability. When the air is stable or neutral this formulation is also used in the rest of the boundary layer. During stable conditions, however, growth of convective plumes is the dominant process and K_z is computed as

$$K_z = kw_*z(1 - \frac{z}{h}) \quad (98)$$

where the convective velocity w_* has replaced the friction velocity. Above the boundary layer K_z is calculated as

$$K_z = K_{z,0} + l^2 \cdot \left| \frac{\Delta v}{\Delta z} \right| \cdot \frac{(R_c - R_b)}{R_c} \quad (99)$$

where $K_{z,0}$ is the background value $1.0 \text{ m}^2\text{s}^{-1}$, l the mixing length, Δv the horizontal wind speed difference across the layer of thickness Δz , R_b the Richardson number and R_c the critical Richardson number given as $R_c = 0.257 \cdot \Delta z^{0.175}$. K_z is set equal to $K_{z,0}$ if the Richardson number gets larger than the critical value. A more detailed description can be found in Strand and Hov (1993) and Flatøy (1994).

The convection is calculated by a modified version of the Asymmetrical Convective model (ACM) by Pleim and Chang (1991). The ACM is a simple non-local closure model for vertical mixing in the convective boundary layer (CBL), based on the assumption that the vertical transport within the CBL is inherently asymmetrical. The ACM simulates the rising buoyant air plumes originating in the surface layer by moving air parcels from the lowest layer directly to the other layers in the CBL. The compensating downward

motion takes place from one layer to the layer below, in order to simulate the slow subsidence surrounding convective plumes. This scheme gives faster upward transport of the surface emission compared to the normal eddy diffusion.

The MCT is designed to study the atmospheric chemical processes in the troposphere and aims at simulating the main parts of the observed tropospheric photochemistry. In this study an extensive bromine and chlorine chemistry and simplified hydrocarbon chemistry with lumped species are used, see section 2.1 and Table 2.

21 different photolysis rates J_i (see Table 3) are computed for each grid box from the function

$$J_i = a_i \exp(-b_i \sec\theta) \quad (100)$$

where θ is the zenith angle and a_i and b_i precomputed values computed by a radiative transfer model. Typical values are given in Table 3.

The dry deposition of O_3 , H_2O_2 , NO_2 , HNO_3 , CH_3O_2H , CO , HCl , $HOCl$, HBr , $HOBr$ and SO_2 is included in the model as a function of latitude, time of day, time of year, biological activity of the surface, surface type and meteorological conditions. The formulations applied are similar to descriptions found in McKeen et al. (1991) and Hass (1991) and maximum deposition velocities over land and sea are given in Table 4. Wet deposition of HNO_3 , SO_2 , H_2O_2 , CH_3O_2H , HCl and HBr is calculated from the rate of precipitation at ground, the rainout rate from each vertical layer available from the numerical weather prediction model, and the wet scavenging coefficient for each species (Table 7).

Specie	λ
HNO_3	1.4×10^6
SO_2	5.0×10^5
H_2O_2	5.0×10^5
CH_3O_2H	5.0×10^5
HCl	1.4×10^6
HBr	1.4×10^6

Table 7: Wet scavenging coefficients applied in the simulation.

Emissions of anthropogenic NO_x and $NMHC$ were taken from the CORINAIR 50·50 km^2 inventory for 1993. In the calculations the anthropogenic $NMHC$ emissions were represented (by volume) as 45% ethane,

30% ethene, 10% ethyne, 10% methanol and 5% formaldehyde. The chemistry and emissions of isoprene end terpenes are not taken into account since their reactions towards halogens are unknown and they are assumed to have only minor direct influence in the marine environment due to their short lifetimes.

7.2 Model results and discussion

Calculations were done for the period 30 April - 10 May 1997 to investigate the competition between chemical and physical processes in the determination of the fate of the halogen radicals, to assess the importance of the various processes that determine the partitioning between different halogenated compounds and the potential role of halogens in the *NMHC*, *NO_x* and ozone chemistry in the marine environment.

Only gas phase chemistry was considered and emissions of *Br₂* and *Cl₂* were equal to 3.5×10^8 and 1.0×10^{10} molecules $cm^{-2}s^{-1}$, respectively, over the sea (no emissions over ice and land). This is the same as used in the box model calculations in section 4, but instead of assuming an instant mixing in the mixing layer, vertical diffusion, vertical advection and convection act to distribute the emission vertically. Constant emission rates were assumed due to lack of more information, but the fate and concentration range of the different halogen compounds over different areas and under different meteorological conditions could then be investigated. Since the main aim of this study is to investigate the relative importance of halogens and their partitioning, zero cloud cover was assumed to facilitate the investigation of the change in chemistry with latitude.

In Figure 15 the mean sea level pressure and wind in model layer 8 (~ 1200 m) are shown.

The period was characterized by a rather weak low pressure system west of Norway and a high pressure ridge in the south Atlantic. Surface winds were very low in the south western part of the model area with winds on average being 2-3 m/s and gusting up to 7-9 m/s. On the other hand winds north west of the UK were on average 8-10 m/s with gusts up to 20 m/s west of Ireland.

Figures 16 and 17 give the average concentration of *BrO*, total gas phase bromine ($BrO_y = Br + 2 \cdot Br_2 + BrO + HBr + HOBr + BrONO_2 + BrCl$), *ClO* and total gas phase chlorine ($ClO_y = Cl + 2 \cdot Cl_2 + ClO + HCl + HOCl + ClONO_2 + 2 \cdot Cl_2O_2 + BrCl$), respectively, in the lowest model

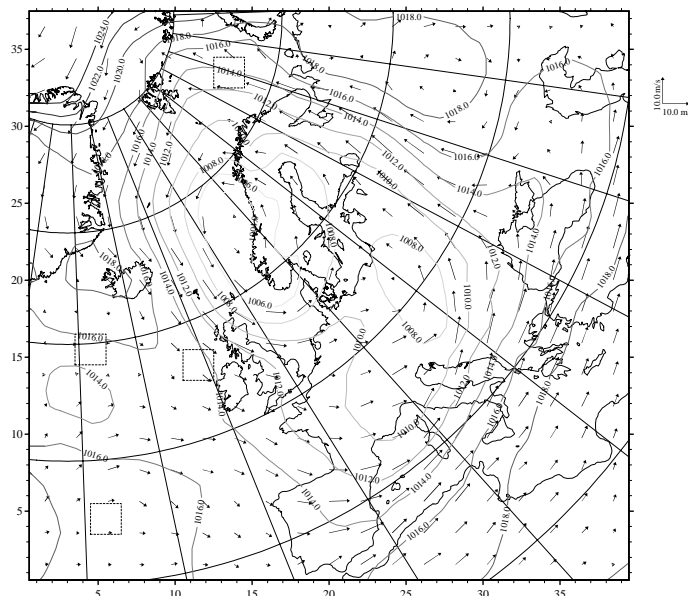


Figure 15: Mean sea level pressure and mean windspeed at model level 8 (~ 1200 m) for model period 30 April - 10 May 1997.

layer (0-90 m) over the model domain when no heterogeneous or aqueous phase reactions were considered. Even if the emissions of halogens were held constant over the sea the average BrO_y and ClO_y concentrations vary with almost an order of magnitude from 3 to 20 ppt and from 70 to 650 ppt, respectively, within the model domain. The highest concentrations were found in the south western part of the model domain. This is explained by low windspeeds and little vertical diffusion in this area allowing a larger portion of the halogens to stay near the surface. A more comprehensive explanation and partitioning of the total bromine and chlorine concentrations into different compounds are given in section 7.3.

Figures 18 to 22 give the average concentration and difference between a run with halogen emissions and one without (with halogens/no halogens) of ozone, $NMHC$, $HCHO$ and NO_x and average 12 GMT concentrations of RO_2 ($HO_2 + CH_3O_2$) in the lowest model layer (0-90 m).

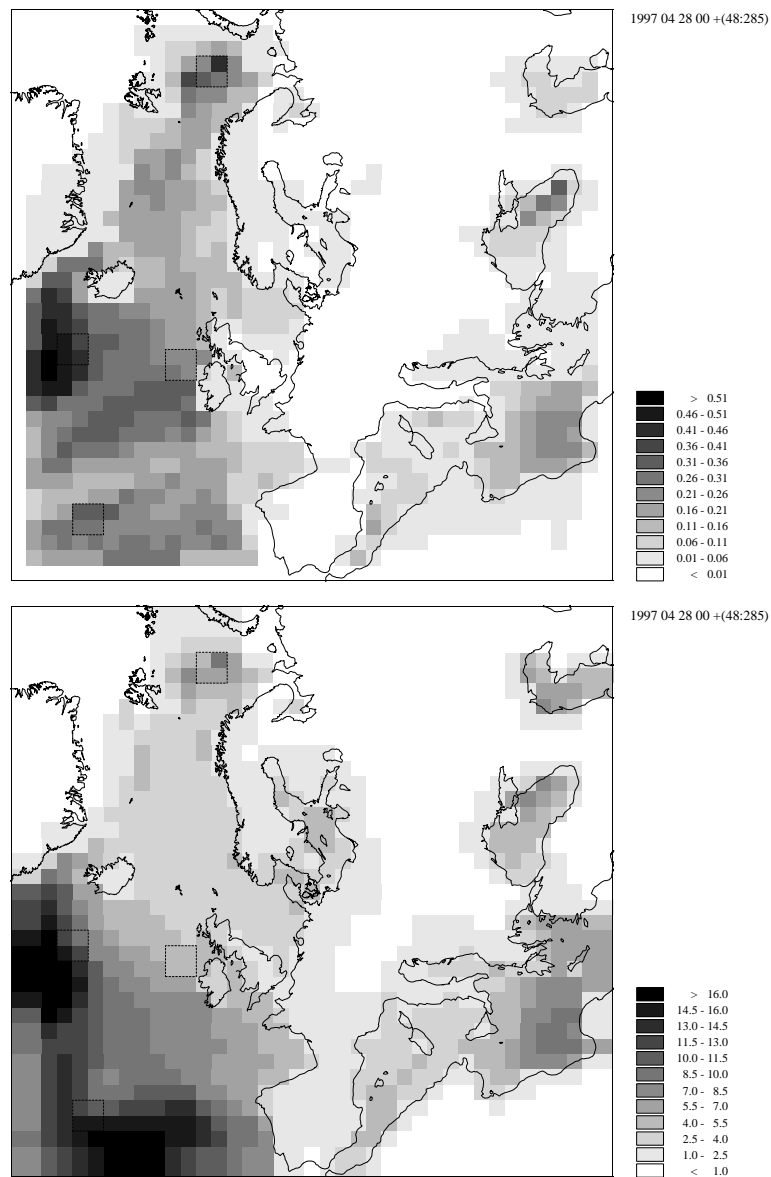


Figure 16: Average BrO (upper) and average BrO_y (lower), (ppt) in the model domain during the model period (30 April - 10 May, 1998) for the lowest model layer (0-90 m). Due to ice north east of Greenland no halogens were emitted in this region.

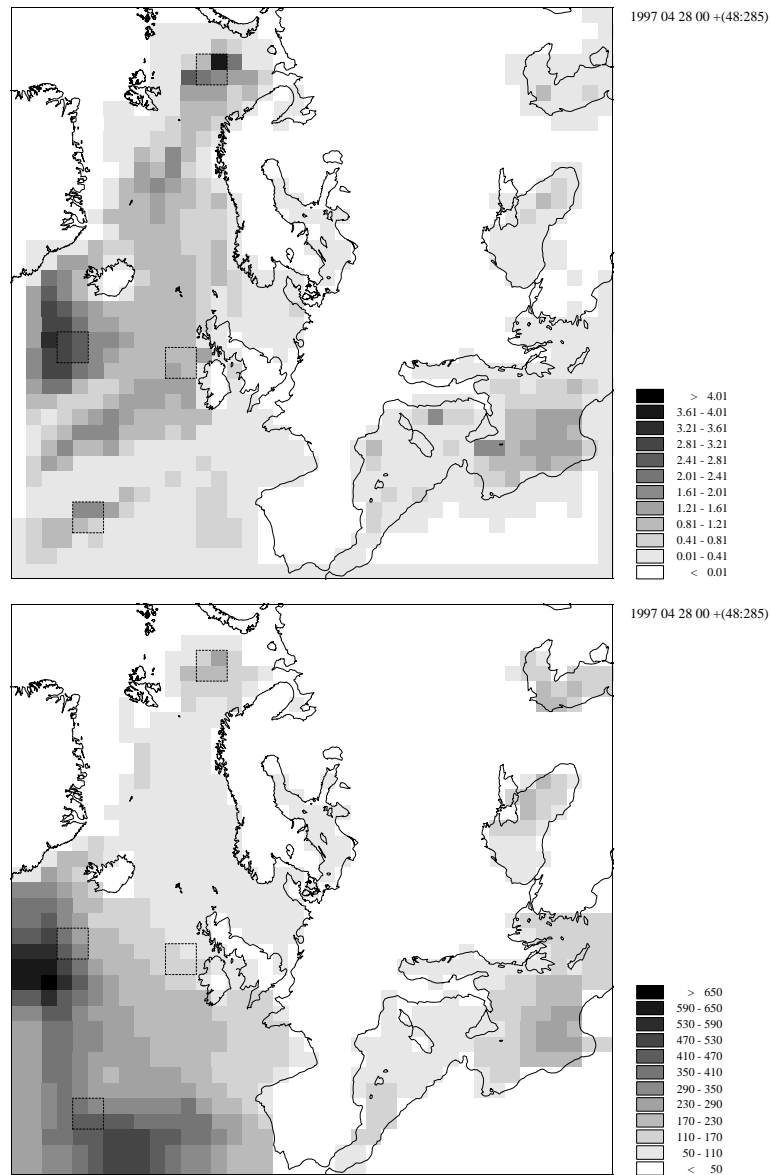


Figure 17: Average ClO (upper) and average ClO_y (lower) (ppt) in the model domain during the model period (30 April - 10 May, 1998) for the lowest model layer (0-90 m). Due to ice north east of Greenland no halogens were emitted in this region.

It is seen that the east and north east Atlantic and the North Sea area are characterized by low concentrations of both primary and secondary pollutants due to the westerly and north westerly winds bringing clean air into this area. As seen in the box model calculations even relatively low halogen concentrations like the one in this calculation may influence the concentration of other species. This is particularly pronounced in the areas with high chlorine concentrations, where on average 15% more of the *NMHCs* are oxidized giving an increase in *HCHO* and daytime *RO₂* of around 30% where the *ClO* and *ClO_y* concentrations are highest. The *ClO* concentrations then peaked up to 10-30 ppt during sunrise. This reduction in *NMHCs* and increase *HCHO* concentrations have also been reported in the literature during arctic ozone depletion events (Ramacher et al., 1997 and De Serves, 1994). Also a large relative reduction of *NO_x* is seen with reductions of around 50% in these areas where *HCHO* and *RO₂* increased. This is mainly due to production of *ClONO₂* from the reaction of *ClO* with *NO₂*. Reduction of *NO_x* in the presence of halogens is supported by observations of *NO_x* reported by Beine et al. (1997) for Arctic conditions. A more thorough description of the halogens influence on other compounds in the different areas is given in section 7.5.

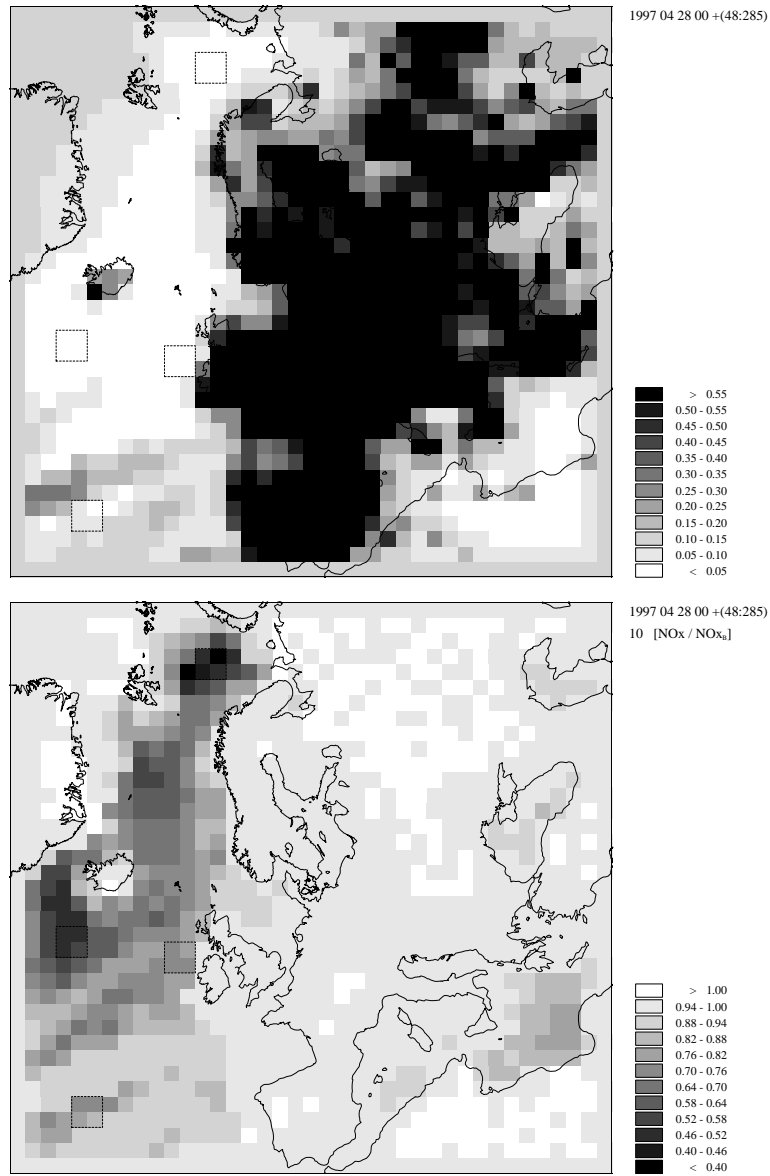


Figure 18: Average NO_x (upper) concentrations in ppb during a model run with halogen emissions and comparisons with a run without halogens (with halogens/no halogens) (lower).

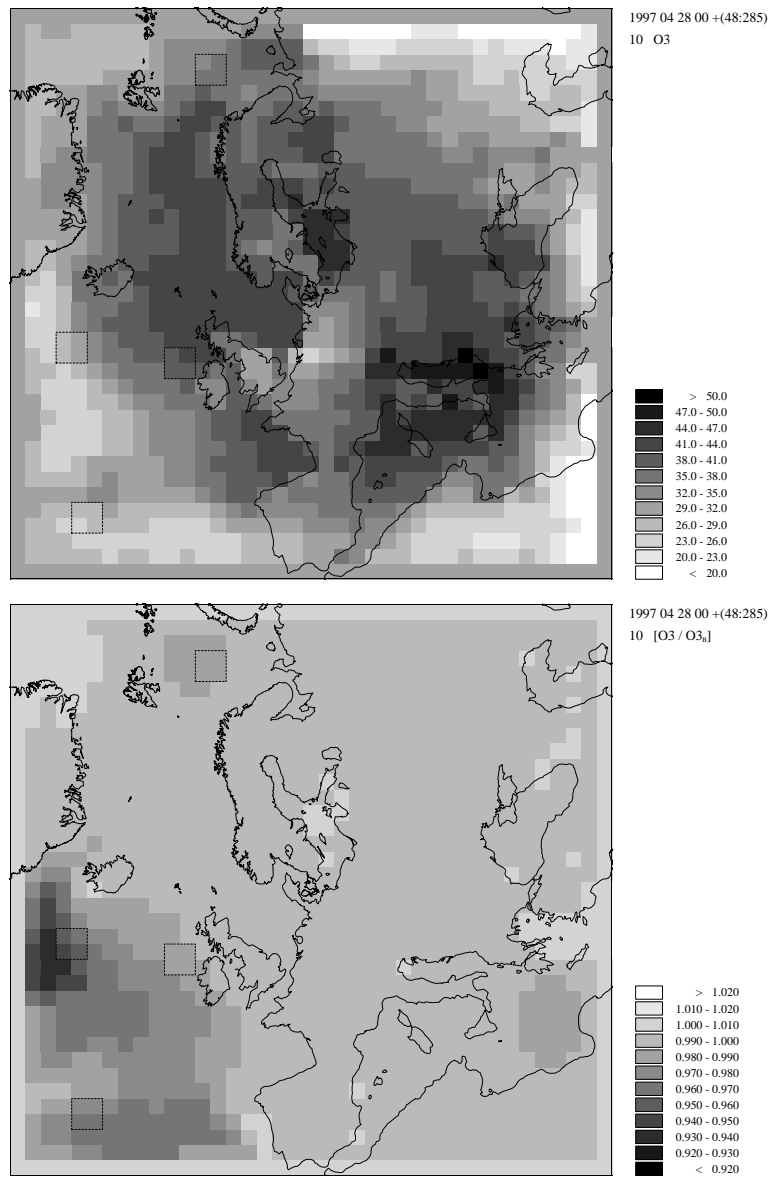


Figure 19: Average ozone (upper) concentrations in ppb during a model run with halogen emissions and comparisons with a run without halogens (with halogens/no halogens) (lower).

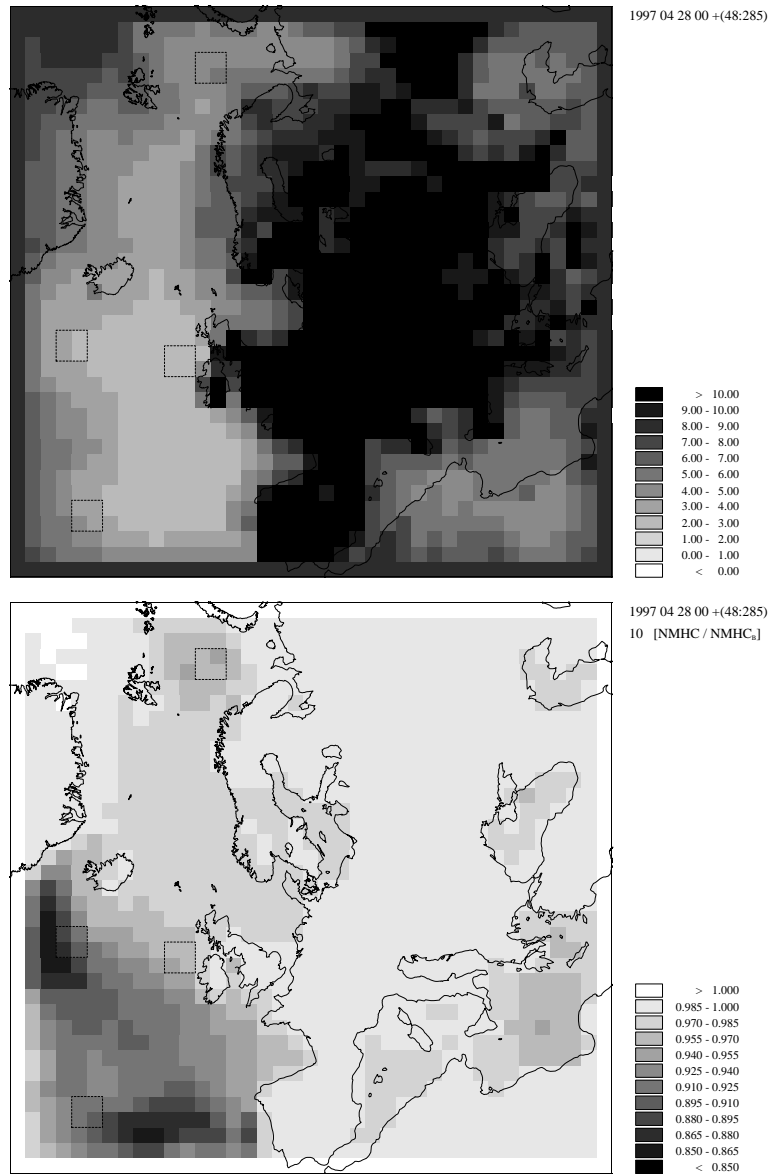


Figure 20: Average *NMHC* concentrations (upper) in ppbC during a model run with halogen emissions and comparisons with a run without halogens (with halogens/no halogens) (lower).

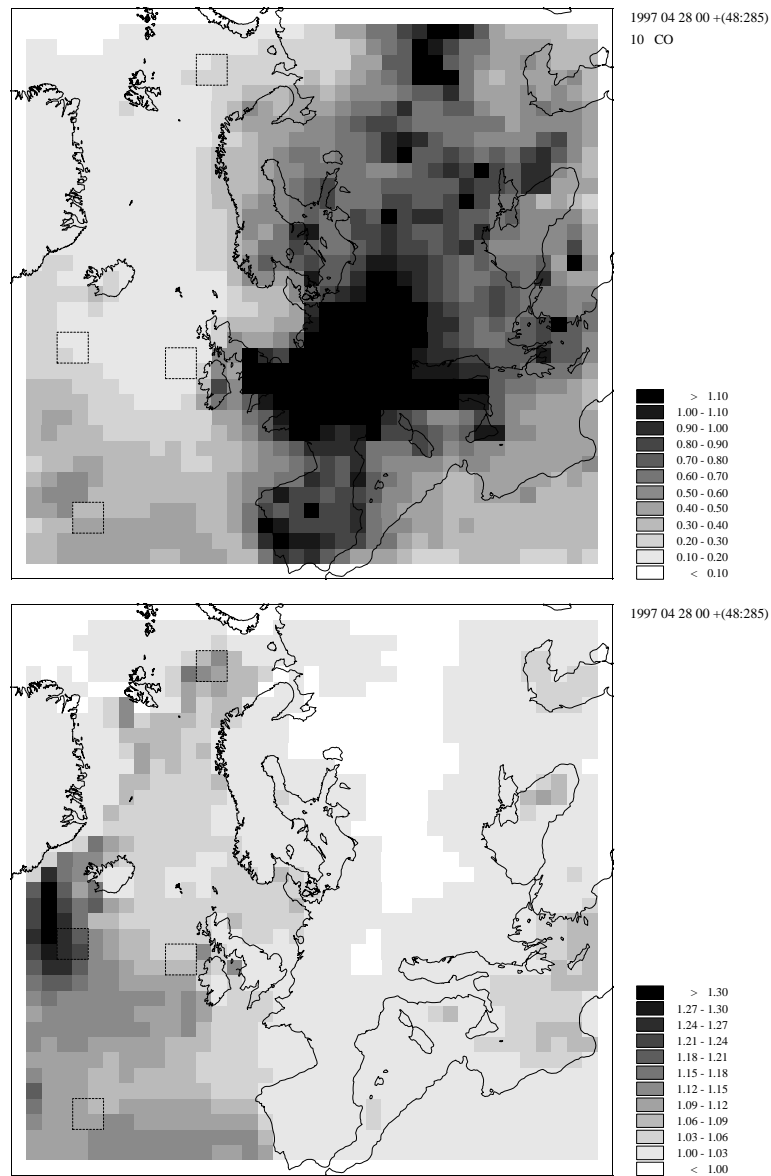


Figure 21: Average $HCHO$ concentrations (upper) (ppb) during a model run with halogen emissions and comparisons with a run without halogens (with halogens/no halogens) (lower).

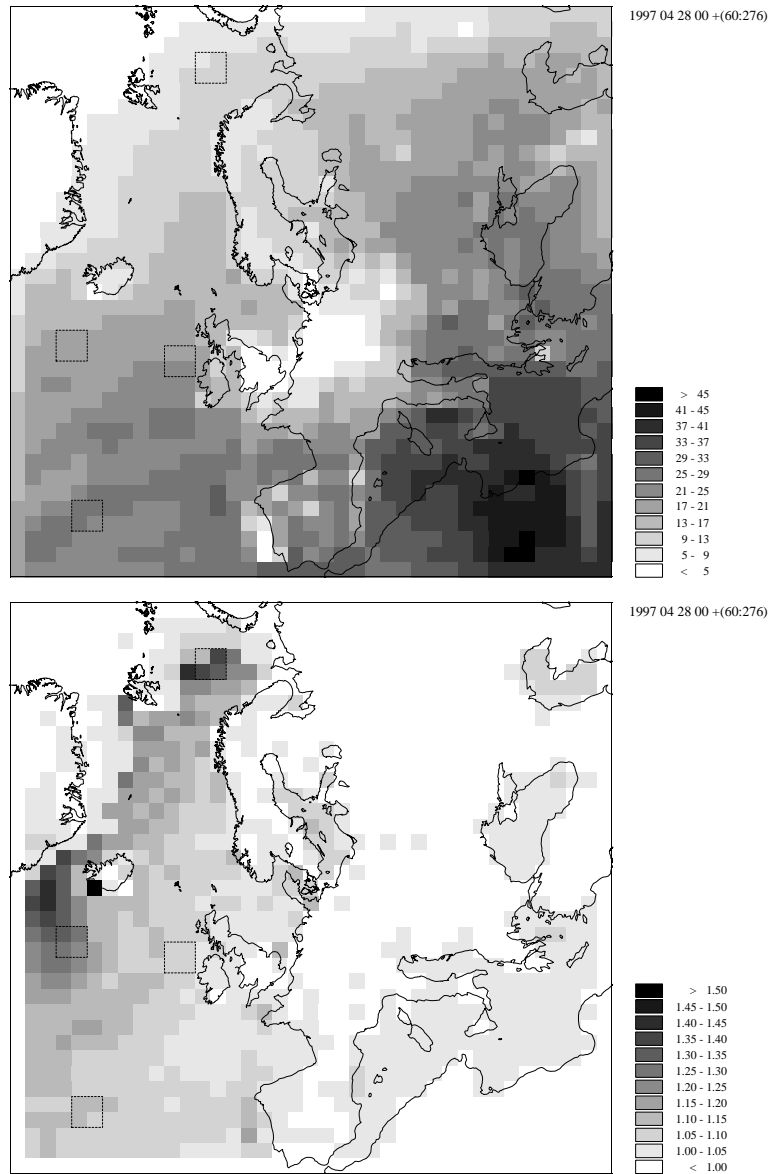


Figure 22: Average 12 GMT RO_2 concentrations (upper) in ppt during a model run with halogen emissions and comparisons with a run without halogens (with halogens/no halogens) (lower).

7.3 Partitioning and concentrations of the halogens over four sub areas.

Four sub areas of the model domain were chosen to show the differences in concentrations and partitioning of the halogens under different NO_x , VOC and ozone concentrations and different meteorological conditions.

All areas were characterized by low NO_x and hydrocarbon loads and quite similar levels of ozone. The windspeeds and temperatures were, however, quite different and this has led to large differences in the mixing of the halogens in the vertical. Figure 15 shows the location of the different areas (2×2 gridcells).

- **Arctic:** Located at approximately 75° N with daytime temperatures around 0° C and an average windspeed of 5 m/s during the model calculation. Characterised by low NO_x (25 ppt), low $NMHC$ (5 ppbC), low RO_2 (12 ppt (average daily maximum)) and 35 ppb of ozone.
- **North Atlantic:** South west of Iceland at 60° N, daytime temperatures around 8° C and average windspeed 3 m/s. Low NO_x (15 ppt), low $NMHC$ (3 ppbC), medium RO_2 (18 ppt (average daily maximum)) and 29 ppb of ozone.
- **West of UK:** West of UK (56° N), daytime temperatures around 8° C and average windspeed 7 m/s. Low NO_x (25 ppt), low $NMHC$ (3 ppbC), medium RO_2 (21 ppt (average daily maximum)) and 40 ppb of ozone.
- **South Atlantic:** West of Spain (45° N), daytime temperatures around 15° C and average windspeed 3 m/s. Low NO_x (60 ppt), low $NMHC$ (4 ppbC), relatively high RO_2 (27 ppt (average daily maximum)) and 27 ppb of ozone.

7.4 Concentrations and partitioning of the halogen compounds

Figure 23 shows the concentrations of total bromine (BrO_y) and chlorine (ClO_y) and the individual bromine and chlorine compounds in the lowest model level for the four different areas.

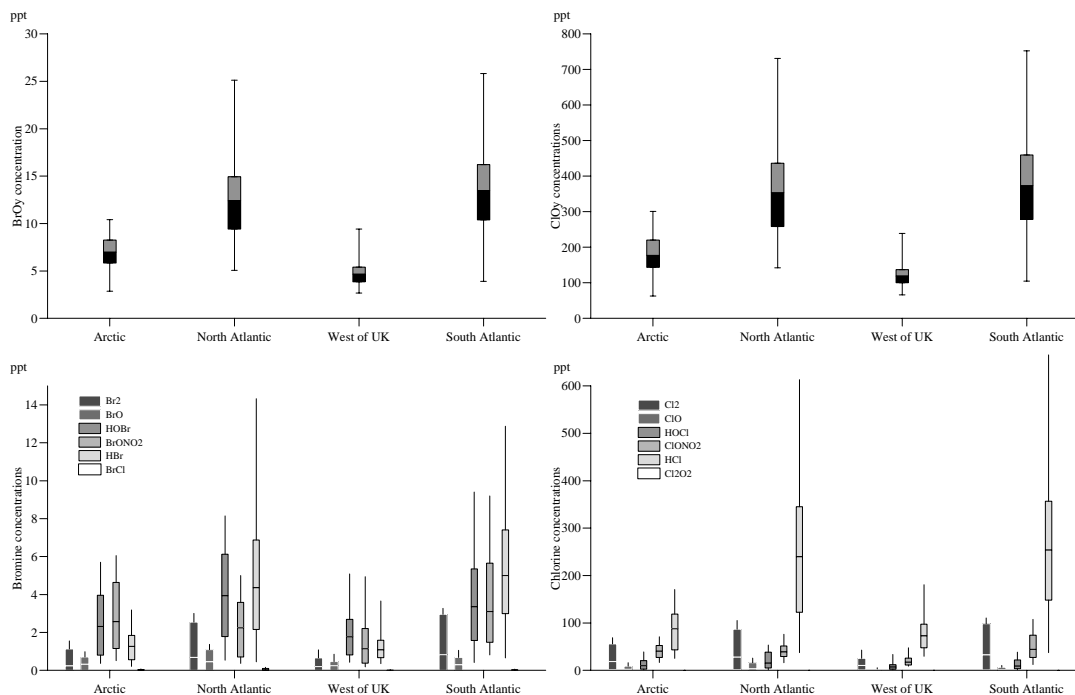


Figure 23: Average, daily average maximum, daily average minimum and maximum and minimum concentrations during the model period for total gas phase bromine (BrO_y , upper left) and chlorine (ClO_y , upper right) in ppt for the lowest model layer, and the concentrations of the individual bromine, (lower left) and chlorine (lower right) compounds (ppt).

The halogen emissions were constant in the calculation. The average BrO_y and ClO_y concentrations vary within a factor of 4 over the different areas, mainly due to differences in the vertical diffusion. This is seen in Figure 24 where the tendency terms in ppt/h for the different meteorological and chemical processes are calculated for the emitted specie Br_2 in the lowest model layer. Negative values indicate loss of the compound. The tendency terms describe chemistry+emission, horizontal advection, vertical advection, diffusion and convection. Due to the formulation of the numerical solution the chemistry and emission tendencies are not separated. On average 0.13 ppt/h is transported out of the lowest model layer by diffusion

in the area west of the UK compared to 0.03 ppt/h in the north and south Atlantic area. This is a factor of about 3 and explains the differences in BrO_y and ClO_y concentrations in the different areas. In addition contributions by vertical and horizontal advection have to be taken into account, but these two terms almost eliminate each other on average within the mixing layer when the emissions are uniformly distributed as here. This is, however, not always the case for shorter periods. It is also seen that the daily average maximum buildup of Br_2 due to emissions are 6-20 times the daily average. The buildup takes place during night and is reduced by photodissociation during daytime and may exceed the emission rates and therefore give a negative emission+chemistry tendency.

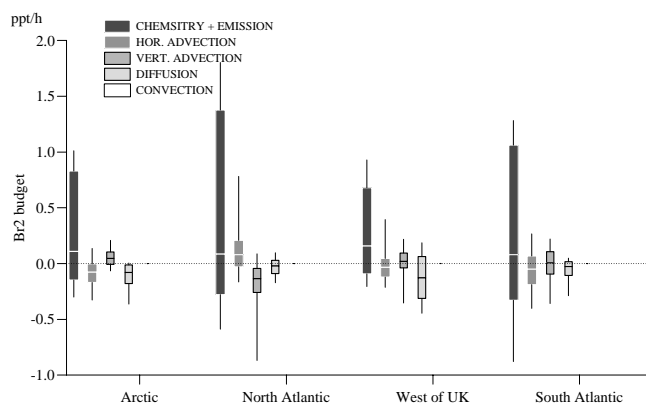


Figure 24: Average, daily average maximum, daily average minimum and maximum and minimum tendencies in ppt/h for the emitted specie Br_2 in the lowest model layer for the period 30 April - 10 May 1997.

Due to higher emission rates and lower photodissociation rates more ClO_y remains as Cl_2 than is the case for BrO_y and Br_2 .

Since HBr and HCl are the two long lived reservoir components of bromine and chlorine in the gas phase, the HBr to BrO_y and HCl to ClO_y ratios express the amount of unreactive compounds available.

Figure 25 shows that HCl is on average 49 to 65% of the total chlorine, and up to 65-83% during daytime.

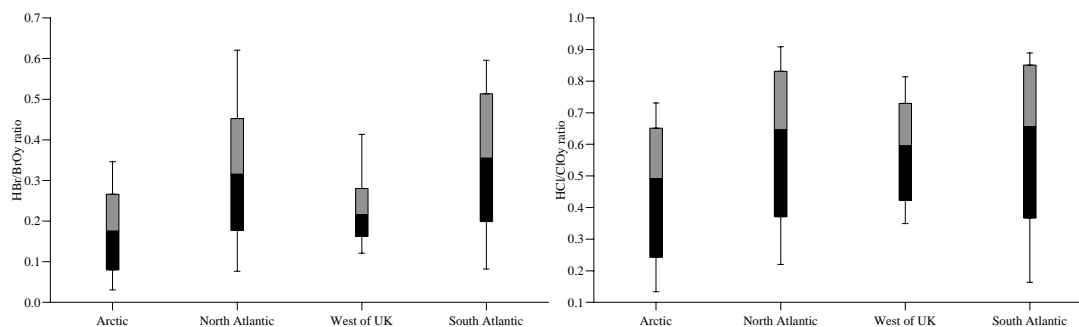


Figure 25: Average, daily average maximum, daily average minimum and maximum and minimum HBr/BrO_y (left) and HCl/ClO_y (right) over the four different areas for the lowest model layer for the period 30 April - 10 May 1997.

Due to much lower reactivity of Br with hydrocarbons, the HBr to BrO_y ratio is only 17 to 35%. The lowest ratio is in the Arctic area. This may be surprising since $NMHC$ and $HCHO$ are higher and OH lower (Figure 28) than in the other areas, favouring HBr production. But the photolysis of $BrONO_2$, $HOBr$ and BrO to Br is much slower in this region ($75^\circ N$), and the production of HBr slower. This is also seen in the BrO to HBr ratio which is about 0.3, more than twice the value in the north and south Atlantic region. The low HBr to BrO_y ratio to the west of the UK is due to low $HCHO$ and $NMHC$ and high ozone concentrations compared to the other areas, favouring production of other bromine species.

Due to the high ozone and low $HCHO$ and $NMHC$ west of the UK, the BrO_x to BrO_y ratio is highest there (Figure 26) on average 6%. This is more than twice the value in the south Atlantic region.

Total bromine (BrO_y) is lowest in the area west of the UK, but the chemical production of BrO is largest, and on average 0.04 ppt/h, 3-5 times the average production in the other regions (Figure 27).

At night there is a net chemical loss of BrO since Br is low. BrO is removed by vertical diffusion to a larger extent than over the other regions and less remains to be chemically converted, causing a large chemical BrO production on average even if the daytime production is larger in all the other areas. The ClO_x to ClO_y ratio resembles that of BrO_x over BrO_y . Only 0.3 to 1% of total chlorine is found as ClO_x on average compared to

2.5-6% for BrO_x . BrO and ClO constitute over 95% of BrO_x and ClO_x .

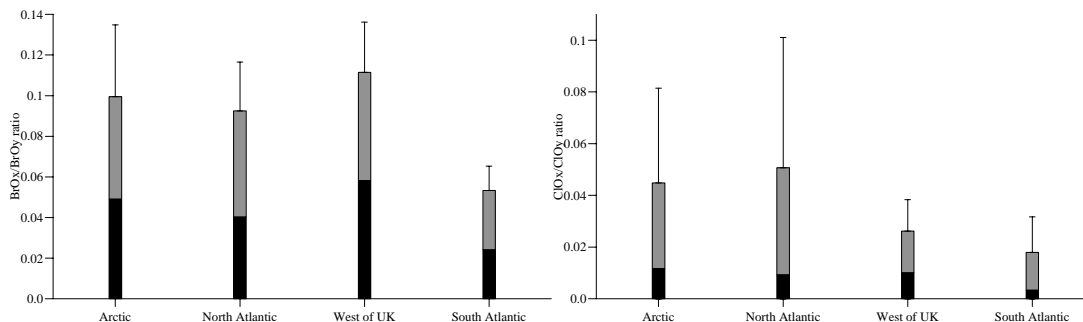


Figure 26: Average, daily average maximum, daily average minimum and maximum and minimum BrO_x/BrO_y (left) and ClO_x/ClO_y (right) over the four different areas for the lowest model layer for the period 30 April - 10 May 1997.

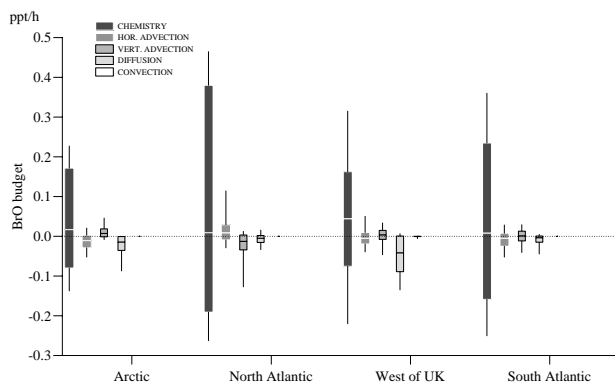


Figure 27: Average, daily average maximum, daily average minimum and maximum and minimum tendencies in ppt/h for BrO over the four different areas for the lowest model layer for the period 30 April - 10 May 1997.

7.5 The halogens influence on other compounds

The halogen emissions were rather small with daily BrO and ClO concentrations of only 0.3-0.5 and 0.5-1.1 ppt, respectively, with peaks up to 1.1-2.9 and 3-16 ppt, they had a pronounced effect on the clean air NO_x ,

NMHC and RO_2 concentrations. Figure 28 shows that all areas have reduced *NMHC* concentrations with 4-10%.

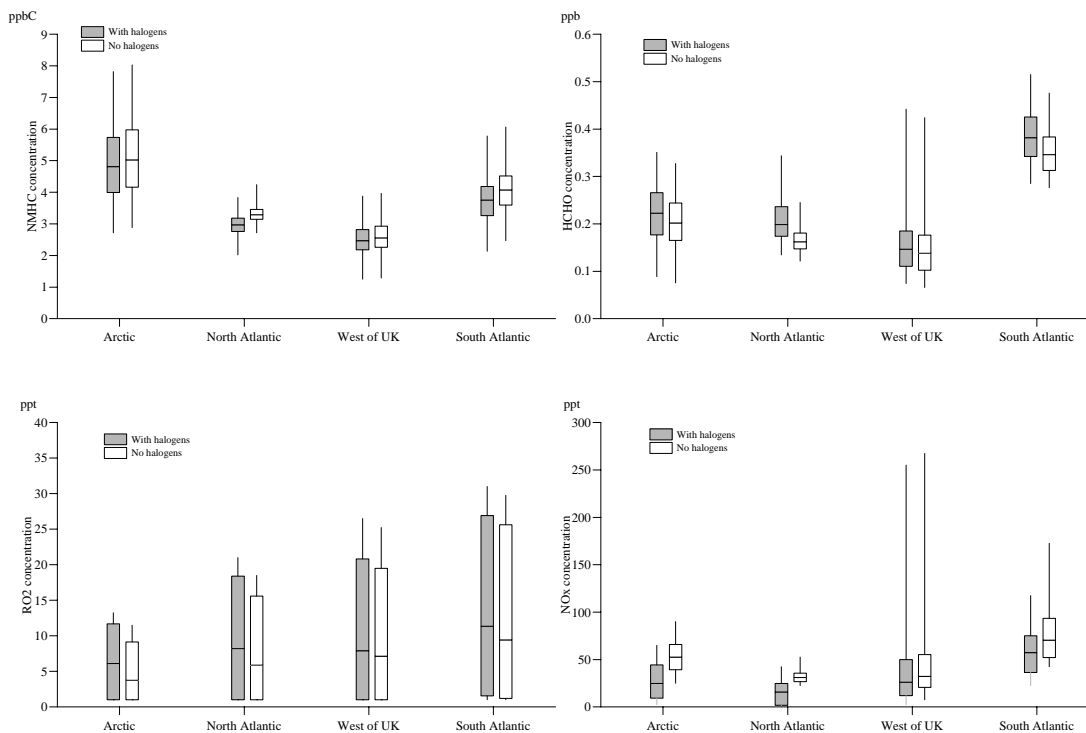


Figure 28: Average, daily average maximum, daily average minimum and maximum and minimum concentration of *NMHC* (upper, left), *HCHO* (upper, right), RO_2 (lower, left) and NO_x (lower, right) with (dark bars) and without (bright bars) halogen emissions for the period 30 April - 10 May 1997.

This increase in oxidation gave higher RO_2 and *HCHO* concentrations. RO_2 increased by 5-28% with the largest increase in the Arctic. The RO_2 concentrations were lowest in the Arctic, and *Cl* reaction with hydrocarbons was most important there. The *Cl* + *NMHC* reactions are temperature dependent, with faster reactions in a cold environment. Most of the

RO_2 increase was due to increase in CH_3O_2 . Due to the increase in peroxy radicals a larger amount of $HCHO$ was produced by the CH_3O_2 self reaction. Also Cl reactions with CH_3O_2 and CH_3OH , and ClO reaction with CH_3O_2 , increased the $HCHO$ concentration. The reduction in average ozone concentrations due to the halogens were less than 1% (Figure29).

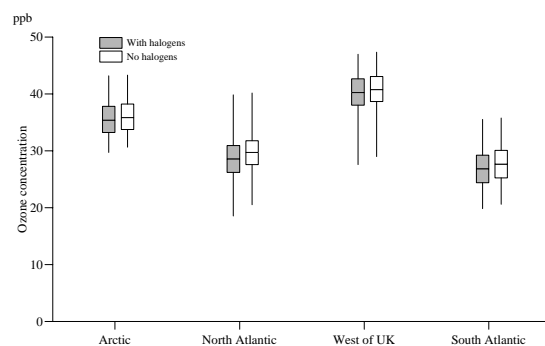


Figure 29: Average, daily average maximum, daily average minimum and maximum and minimum concentration of ozone with (dark bars) and without (bright bars) halogen emissions for the period 30 April - 10 May 1997.

8 Observations and model results

Most observations of tropospheric halogens are done in the Arctic environment (Hausmann and Platt, 1994; Tuckermann et al., 1997) and may not be directly comparable to the values calculated in this study, but they give an indication of the range of concentrations of halogens that might be found in the boundary layer. Table 8 summarizes observations of bromine and chlorine oxide and model calculations reported in this paper. The calculations reported here are within observed range of values for most cases.

There are few other measurements of other gas phase bromine and chlorine compounds, but Perner et al. (1997) measured total gas phase bromine analysed by neutron activation during the ARCTOC 1996 cam-

Measurement campaign	<i>BrO</i>			<i>ClO</i>			Event type
	AVG	PEAK	D.L.	AVG	PEAK	D.L.	
Measurements							
Polar Sunr. ¹	< 2.5	6	4				normal ozone
ARCTOC 1995 ²	0.5	4	1.5	1.6	10	18	normal ozone
ARCTOC 1996 ²	0.8	7	1.5	1.3	10	4.5	normal ozone
Weybourne ³	0.035	3	2.6	1.5	30	14	normal ozone
Mace Head ⁴	-0.2	4.4	1.7				normal ozone
This model study							
Box, clean air	1.0	2.3		4.5	19		normal ozone
3-D	0.3-0.5	0.9-1.4		1.1-2.9	6-26		normal ozone
Measurements							
Polar Sunr.	12	17	4				Low ozone
ARCTOC 1995	15	30	1.5	21	40	18	Low ozone
ARCTOC 1996	3.5	22	1.5	3.3	15	4.5	Low ozone
This model study							
Box, clean air	7.0	29		1.3	10		Low ozone

Table 8: Average (AVG), peak levels (PEAK) and detection limit (D.L.) of measurements of *BrO* and *ClO* during periods of normal and low ozone concentrations. Model calculations from box model calculations (clean air case) and 3-D simulations done in this paper. The values cited for the 3-D simulations is the concentration range for the four sub areas. ¹ Arctic polar sunrise experiment in Alert (1992), ² Arctic polar sunrise experiment in Ny Ålesund, ³Northfolk, UK (1996), ⁴western Ireland (1997).

paign, bromine to be around 10-20 ppt during normal ozone conditions. This is not directly comparable to the total gas phase bromine given in this study since organic bromine is not accounted for in the model, but in the 3-D calculations average *BrO_y* ranged from 7-13 ppt in the four different sub areas. In the box model for the clean air case *BrO_y* was calculated to build up to 40 ppt after two days and to 60 ppt after five. Total gas phase bromine levels were reported to be about three times the *BrO* level during low ozone events (Perner et al., 1997). The box model of *BrO_y* in the clean air case are on the average about six times higher than the *BrO* concentration during a ozone depletion event. The higher *BrO_y* concentrations in the box model may be due to underestimation of a surface sink of *HBr* and *HOBr*, or no wet deposition in the box model runs and diffusion and advection were not accounted for in these calculations.

9 Conclusions

Box model calculations were carried out to investigate the influence of halogens on ozone in polluted and clean air. The effect on ozone was similar in both cases. A small ozone reduction was seen due to reaction with *Br*. The clean air *ClO* concentrations peaked at 2-3 times the value in the polluted case for the same emissions of halogens. The *BrO* concentration did not show much difference between the two cases because the higher *BrO* production in the polluted case was balanced by a larger loss through reaction with *HO₂* and *CH₃O₂*. In the polluted case *HOBr* and *BrONO₂* concentrations were enhanced on the expense of *HBr* compared to the case in cleaner air.

Increased *Cl₂* emissions did not increase the loss of ozone in a linear way, but went through a maximum whereafter the net loss of ozone dropped, mainly due to the change in the $BrO + ClO \rightarrow Br + ClO + O(^3P)$ reaction where the net ozone loss is zero, but it is three times faster than the *BrO* self reaction, and the ozone destruction is reduced by this reaction. In addition the increased peroxy radical concentrations from the chlorine oxidation of *NMHC* may increase the production of ozone. Large peroxy radical concentrations indirectly increase the conversion of active *Br* into inactive *HBr* through the formation of *HCHO*, which is quite reactive towards *Br*.

Release of halogens through liquid sea salt aerosols, and sea salt aerosols as a source for gas phase halogens were investigated. Prescribed accommodation coefficients were used in box model calculations of ozone depletion in polluted and clean air. Depending on the liquid water content, the scavenging of *HOX*, *XONO₂* and *HX* ($X = Br$ or Cl) by liquid sea salt aerosols and consequent release of *Br₂* may deplete ozone completely within a day under optimal conditions. *BrO* concentrations peaked at 95 and 30 ppt in the polluted and clean air cases, respectively. The differences in *BrO* levels were due to the different amounts of ozone depleted (100 and 30 ppb, respectively). Free radicals may be scavenged by aerosols and react with sea salt bromine and act as a source of gas phase bromine. This process was investigated and shown not to make a large contribution due to the slow scavenging, but can activate *HOBr* in sea salt.

The products of reactions of type $Br + NMHC$ were investigated. The fate of these products determine the bromine ozone destruction potential. This was especially the case for the products of the reaction $Br + HCHO$.

BrO can be a significant sink of *DMS* even at *BrO* concentrations of about 2 ppt. *DMS* was calculated to be almost totally depleted during ozone depletion events.

3D CTM model runs were done for the period 30 April to 10 May, 1997 over Europe and the North Atlantic. The period was characterized by clean air over the sea with small amounts of *NMHC* and *NO_x* in the range of 2-6 ppbC and 25-100 ppt, respectively. The emissions of halogens were held constant over the sea in order to investigate the differences in concentration levels do to mixing processes. *BrO_y* and *ClO_y* concentrations in the lowest model level varied with almost an order of magnitude within the model domain due to differences in vertical diffusion. This shows that physical processes are important for the halogen concentrations, and observed increases in concentration may often not indicate increased emissions.

HCl was seen to be by far the most important *ClO_y* component and accounted for more than 50% of total *ClO_y* even if the hydrocarbon loads were quite small. In contrast, *HBr* accounted for about 20% of total *BrO_y*. Chlorine is thus much faster deactivated if no heterogenous or aqueous phase reaction reactivates *HCl*. The partitioning of the different bromine species was more similar than in the chlorine case and in some areas both *HOBr* and *BrONO₂* exceeded the *HBr* concentration on average.

ClO concentrations of a few ppt as a daily average, and with maxima of 10-30 ppt during daytime, oxidized 10-15% more of the *NMHC*s compared to a run without halogens. This increased the daytime peak of *RO₂* with 15-30% and increased the *HCHO* concentration on average 10-20%. The halogens were shown to have little effect on ozone (1-4% reduction) due to the low amounts of bromine peaking up to about 1 ppt. *NO_x* levels were greatly reduced in the halogen emission case by the *ClO* reaction with *NO₂*, in some areas up to 50% compared to the run without halogens. Chlorine may therefore be an important sink of *NO₂* in areas where the photodissociation of *ClONO₂* is slow.

Acknowledgement: The work reported here was funded by the EU Commission through the projects ARCTOC, HALOTROP-CYMFO and TACIA.

References

- Anderson G.P., Clough S.A., Kneizys F.X., Chetwynd J.H. and Shettle E.P.** (1986) AFGL Atmospheric Constituent profiles (0-120 km). *AFGL-TR-860110, AFGL (OPI), Hanscom AFB, MA 01736.*
- Barnes I., Bastian V., Becker R.H. and Overath R.D.** (1991) Kinetic studies of the reactions of *IO*, *BrO* and *ClO* with *DMS*. *Int. J. Chem. Kin.*, Vol. 23, pp. 579-591.
- Barrie L.A., Bottenheim J.W., Schnell R.C., Crutzen P.J. and Rasmussen R.A.** (1988) Ozone destruction and photochemical reactions at polar sunrise in the lower Arctic atmosphere. *Nature* 334, pp. 138-141.
- Beine H.J., Jaffe D.A., Stordal F., Engardt M., Solberg S., Schmidbauer N. and Holmen K.** (1997) *NO_x* during ozone depletion events in the Arctic troposphere at Ny Ålesund, Svalbard. *Tellus*, Vol 49B, pp. 556-565.
- Bott A.** (1989) A positive definite advection scheme obtained by nonlinear renormalization and fluxes. *Mon. Wea. Rev.*, 117 1006-1015.
- Bottenheim J., Barrie L., Atlas E., Heidt L. E., Niki H., Rasmussen R. A. and Shepson P. B.** (1990) Depletion of lower tropospheric ozone during Arctic spring: The Polar Sunrise experiment 1988. *J. Geophys. Res.*, Vol 95, pp. 18555-18568.
- Burkholder J.B., Ravishankara A.R. and Solomon S.** (1995) UV/visible and IR absorption cross sections for *BrONO₂*. *J. of Geophys. Res.*, Vol 100, pp. 16793-16800.
- Businger J.A., Wyngaard J.C., Izumi Y. and Bradley E.F.** (1971) Flux profile relationships in the atmospheric surface layer. *J. Atm. Sci.*, Vol. 28, pp. 181-185.
- Chameides W.L. and Stelton A.W.** (1992) Aqueous phase chemical processes in deliquescent sea salt aerosols: A mechanism that couples the atmospheric cycles of S and sea salt. *J. of Geophys. Res.*, Vol. 97, pp. 20565-20580.
- Chang J. S., Brost R. A., Isaksen I. S. A., Madronich S., Middleton P., Stockwell W. R. and Walcek C. J.** (1987) A three-dimensional Eulerian acid deposition model: Physical concepts and formulation. *J. Geophys. Res.*, 92, D12, 14681-14700.
- Cicerone R.J., Heidt L.E. and Pollock W.H.** (1988) Measurements of atmospheric methyl bromide and bromoform. *J. Geophys. Res.*, Vol. 93,

pp. 3745-3749.

Class T., Kohnle R. and Ballschmiter K. (1986) Chemistry of organic trace gases in air VII: Bromo- and bromochloromethanes in air over the Atlantic Ocean. *Chemosphere*, Vol. 15, pp. 429-436.

de Serves C. (1994) Gas phase formaldehyde and peroxide measurements in the Arctic atmosphere. *J. of Geophys. Res.*, Vol. 99, pp. 25391-25398.

Deister U. and Warneck P. (1990) Photooxidation of SO_3^{2-} in aqueous solution. *J. Phys. Chem.*, Vol. 94, pp. 2191-2198.

Fan S.M. and Jacob D.J. (1992) Surface ozone depletion in Arctic spring sustained by bromine reactions on aerosols. *Nature*, Vol. 359, pp. 522-524.

Flatøy F. (1994) Modeling of coupled physical and chemical processes in the troposphere over Europe. *Dr. Scient dissertation, Geophysical. Inst., Univ. of Bergen, N-5007 Bergen, Norway.*

Flatøy F. (1992) Comparison of two parameterization schemes for cloud and precipitation processes. *Tellus 44A*, 41-53.

Fuchs N.A. and Sutugin A.G. (1971) High dispersed aerosols. *Topics in the current aerosol reseach. Ed. Hidy and Brock, pp. 1-60, Pergamon Press, New York.*

Garcia R. and Solomon S. (1994) A new numerical model of the middle atmosphere: 2 - Ozone and related species. *J. of Geophys. Res.*, Vol 99, pp. 12937-12951.

Grønås S., Foss A. and Lystad M. (1987) Numerical simulations of polar lows in the Norwegian Sea. *Tellus 39A*, 224-253.

Hanson D.R., Burkholder J.B., Howard C.J. and Ravishankara A.R. (1992) Measurements of OH and HO_2 radical uptake coefficients on water and sulphuric acid surfaces. *J. Phys. Chem.*, Vol. 96, pp. 4979-4985.

Hass H. (1991) Description of the EURAD Chemistry-Transport-Model Version 2 (CTM2). *Mitteilungen aus dem Institut für Geophysik und Meteorologie der Universität zu Köln, Heft 83.*

Hausmann M. and Platt U. (1994) Spectroscopic measurements of bromine oxide and ozone in the high Arctic during Polar Sunrise Experiment 1992. *J. Geophys. Res.*, Vol. 99, pp. 25,399-25,414.

Jobson B. T., Niki H., Yokouchi H., Bottenheim J., Hopper F. and Leitch R. (1994) Measurements of $C_2 - C_6$ hydrocarbons during the polar sunrise 92 experiment. Evidence for Cl -atom and Br -atom chemistry. *J. Geophys. Res.*, Vol 99, pp. 25355-25368.

- Kvamstø N. G.** (1992) Implementation of the Sundqvist scheme in the Norwegian Limited Area Model. *Meteorological report series, 2-92, Dep. of Geophys., Univ. of Bergen. 5007 Bergen, Norway.*
- Kylling A., Stamnes K., Tsay S.C.** (1995) A reliable and efficient 2-stream algorithm for spherical radiative transfer - Documentation of accuracy in realistic layered media. *J. of Atmospheric Chemistry, Vol. 21, No 2 pp. 115-150.*
- Lary D.J.** (1996) Gas phase atmospheric bromine photochemistry. *J. of Geophys. Res., Vol 101, pp. 1505-1516*
- Lary D.J., Chipperfield M.P., Toumi R. and Lenton T.** (1996) Heterogeneous atmospheric bromine chemistry. *J. of Geophys. Res., Vol 101, pp. 1517.*
- Li S.M., Yokouchi Y., Barrie L.A., Muthuramu K., Shepson P.B., Bottenheim J.W., Sturges W.T. and Landsberger S.** (1994) Organic and inorganic bromine compounds and their compositions in the Arctic troposphere during polar sunrise. *J. Geophys. Res., Vol. 99*
- Lugg G.A.** (1968) Diffusion coefficients of some organic and other vapors in air. *Anal. Chem., 40, pp 1072-1077.*
- Marrero T.R. and Mason E.A.** (1972) Gaseous diffusion coefficients. *J. Chem. Ref. Data, 1 pp. 3-118.*
- McDonnel J.C., Henderson G.S., Barrie L., Bottenheim J., Niki H., Langford C.H. and Templeton E.M.J.** (1992) Photochemical bromine production implicated in Arctic boundary layer ozone depletion. *Nature, Vol. 355, pp. 150-152.*
- McKeen S. A., Hsie E.-Y., Trainer M., Tallamraju R. and Liu S. C.** (1991) A regional model study of the ozone budget in the eastern United States. *J. Geophys. Res., 96, 10809-100845.*
- Mellouki A., Talukdar R.K. and Howard C.J.** (1994) Kinetics of the reaction of *HBr* with ozone and *HO₂*: The yield of *HBr* from *HO₂ + BrO*. *J. of Geophys. Res., Vol 99, pp. 22949-22954.*
- Minschwaner K., Salawitch R.J. and McElroy M.B.** (1993) Absorption of solar radiation by *O₂*: Implications for *O₃* and lifetimes of *N₂O*, *CFCl₃* and *CF₂Cl₂*. *J. Geophys. Res., Vol 98, pp. 10543-10561.*
- Morris E. D. and Niki H.** (1973) Reaction of dinitrogen pentoxide with water. *J. Phys. Chem., 77 1992 -2002*
- Mozourkewich M.** (1995) Mechanisms for release of halogens from sea-salt particles by free radical reactions. *J. of Geophys. Res., Vol. 100, pp.*

14199-14207.

Nordeng T. E. (1986) Parameterization of physical processes in a three-dimensional numerical weather prediction model. *Technical Report No. 65*, DNMI, Oslo, Norway.

Perner D., Trautmann A. and Zauner H. (1996) Measurements of atmospheric halogens by neutron activation. *Arctic Tropospheric Ozone Chemistry (ARCTOC): Final report*, Ed. Platt U. and Lehrer E. Commission of European Communities, Brussels.

Platt U. (1998) HALOTROP-CYMFO Final report to the European Commission. *In preparation*

Pleim J. E. and Chang J. S. (1992) A non-local closure model for vertical mixing in the convective boundary layer. *Atmospheric Environment*, 26, 965-981.

Poulet G., Pirre M., Maguin F., Ramaroson R. and LeBras G. (1992) The role of the $HO_2 + BrO$ reaction in the stratospheric chemistry of bromine. *Geophys. Res. Lett.*, Vol. 19, pp. 2305-2308.

Ramacher B., Rudolph J. and Koppmann R. (1997) Hydrocarbon measurements in the spring Arctic troposphere during the ARTOC 95 campaign. *Tellus*, Vol 49B, pp. 446-485.

Sander R. and Crutzen P.J. (1996) Model study indicating halogen activation and ozone destruction in polluted air masses transported to the sea. *J. of Geophys. Res.*, Vol. 101, pp. 9121-9138.

Schall C., Laturus F. and Heumann K.G. (1994) Biogenic volatile organoiodine and organobromine compounds released from polar macroalgae. *Chemosphere*, Vol. 28, pp. 1315-1324.

Schwartz S.E. (1986) Mass transport considerations pertinent to aqueous phase reactions of gases in liquid water clouds. *Chemistry of multiphase systems*, NATO ASI Ser., Vol G6, Ed. W Jaeschke, pp. 415-471, Springer Verlag, New York.

Sherwood T.K., Pigford R.L. and Wilke C.R. (1975) *Mass transfer*. McGraw-Hill, New York.

Solberg S., Schmidbauer N., Semb A., Stordal F. (1996) Boundary layer ozone depletion as seen in the Norwegian Arctic Spring. *J. Atm. Chem.*, Vol 23, pp. 301-332.

Strand A. and Hov Ø. (1993) A two dimensional zonally averaged transport model including convective motions and a new strategy for the numerical solution. *J. Geophys. Res.*, 98, 9023-9037.

- Sturges W.T. and Harrison R.M.** (1986) Bromine in marine aerosols and the origin, nature and quantity of natural atmospheric bromine. *Atmos. Environ.*, Vol 20, pp. 1485-1496.
- Sundqvist H., Berge E. and Kristjanson J. E.** (1989) Condensation and cloud parameterization studies with a mesoscale NWP model. *Mon. Wea. Rev.*, 117, 1641-1657.
- Sundqvist H.** (1988) Parameterization of condensation and associated clouds in models for weather prediction and general circulation simulations. *Physical based modelling and simulation of climate and climatic change* (ed. M. E. Schlesinger), Reidel, Dordrecht, 433-461.
- Thomas K., Voltz-Thomas A. and Kley D.** (1993) Zur Wechselwirkung von NO_3 Radikalen mit wässrigen Lösungen: Bestimmung des Henry und des Massenakkommodationskoeffizienten. *Ph.D. thesis, Inst. für Chemie und Dynamik der Geosphäre 2, Forschungszentrum Jülich GmbH, Germany.*
- Toumi R.** (1994) BrO as a sink for dimethylsulphide in marine atmosphere. *Geophys. Res. Lett.*, Vol. 21, pp 117-120.
- Tuckermann M., Ackermann R., Golz C., Lorenzen-Schmidt, H., Senne T., Stultz J., Trost B., Unold W. and Platt U.** (1997) DOAS observation of halogen radical-catalysed Arctic boundary layer ozone destruction during the ARCTOC campaigns 1995 and 1996 in Ny Ålesund, Spitsbergen. *Tellus*, Vol 49B, pp. 533-555.
- van Doren J.M, Watson L.R., Davidovits P., Worsnop D.R., Zahniser M.S. and Kolb C.E.** (1990) Temperature dependence of the uptake coefficients of HNO_3 , HCl and N_2O by water droplets. *J. Phys. Chem.*, Vol. 94, pp. 3265-3269.
- Vogt R., Crutzen P. J. and Sander R.** (1996) A mechanism for halogen release from sea-salt aerosol in the remote marine boundary layer. *Nature*, Vol 389, pp 327-330.